TRANSPORTATION RESEARCH RECORD 849

Symposium on Aspects of Subsurface Drainage Related to Pavement Design and Performance

TRANSPORTATION RESEARCH BOARD

NATIONAL RESEARCH COUNCIL

NATIONAL ACADEMY OF SCIENCES
WASHINGTON, D.C. 1982

Transportation Research Record 849
Price $6.00
Edited for TRB by Naomi Kassabian

mode
1 highway transportation

subject area
63 soil and rock mechanics

Library of Congress Cataloging in Publication Data
Symposium on Aspects of Subsurface Drainage Related to Pavement Design and Performance (1982 : Washington, D.C.)
Symposium on Aspects of Subsurface Drainage Related to Pavement Design and Performance.

(Transportation research record; 849)
1. Road drainage–Congresses. 2. Pavements–Congresses. 3. Subsurface drainage–Congresses. I. National Research Council (U.S.). Transportation Research Board. II. Title. III. Series.
TE.H5 no. 849 [TE215] 380.5s [625.7'34] 82-14323
ISBN 0-309-03352-7 ISSN 0361-1981

Sponsorship of the Papers in This Transportation Research Record

GROUP 2–DESIGN AND CONSTRUCTION OF TRANSPORTATION FACILITIES
R. V. LeClerc, consultant, Olympia, Washington, chairman

Soil Mechanics Section
Lyndon H. Moore, New York State Department of Transportation, chairman

Committee on Subsurface Drainage
Lyle K. Moulton, West Virginia University, chairman
Robert G. Carroll, Jr., Barry J. Dempsey, Eugene B. Drake, Wilbur M. Haas, William E. Harrison, Kent A. Healy, Gary L. Hoffman, S. Bennett John, Gary L. Klinedinst, B. Dan Marks, John E. Merten, S. Paul Miller, Lyndon H. Moore, Lee Murch, Willard G. Puffer, Hallas H. Ridgeway, George W. Ring III, Gary A. Shepherd, William D. Trolinger, Hugh L. Tyner, Walter C. Waidelich, Clayton E. Warner, David C. Wyant, Thomas F. Zimmie

John W. Guinnee, Transportation Research Board staff

The organizational units, officers, and members are as of December 31, 1981.

Contents

Authors of the Papers in This Record

Dempsey, Barry J., Department of Civil Engineering, University of Illinois, Urbana, IL 61801
Hoffman, Gary L., Bureau of Contract Quality Control, Pennsylvania Department of Transportation, P.O. Box 2926, Harrisburg, PA 17120
MacMaster, J.B., Highway Engineering Division, Ministry of Transportation and Communications, Downsview, Ontario M3M 1J8, Canada
Markow, Michael J., Department of Civil Engineering, Room 1-230, Massachusetts Institute of Technology, Cambridge, MA 02139
Phang, W.A., Research and Development Branch, Ministry of Transportation and Communications, Downsview, Ontario M3M 1J8, Canada
Raad, Lutfi, Faculty of Engineering, American University of Beirut, New York, NY 10017
Wrong, G.A., Highway Engineering Division, Ministry of Transportation and Communications, Downsview, Ontario M3M 1J8, Canada

Laboratory and Field Studies of Channeling and Pumping

BARRY J. DEMPSEY

Conditions that cause pumping and channeling in pavement systems were studied in the laboratory and the field. Laboratory pavement model tests indicated that dense-graded crushed-stone base courses would experience channeling and pumping under dynamic loading conditions. An open-graded crushed-stone base did not pump, but subgrade intrusion caused permanent deformation of the pavement slab. The University of Illinois test track was used to study six asphalt concrete pavement systems and four PCC pavement systems. It was found that asphalt concrete pavements on both the nonstabilized and bituminous stabilized open-graded layers performed well under repeated wheel loads. The pavement on a well-graded crushed-stone base displayed the poorest performance. The PCC pavement slab on an open-graded base course did not pump, whereas that on a dense-graded base course displayed residual and dynamic pore-water pressures that led to pumping. Field investigations show that pumping continues to be a problem in pavements. However, it is indicated that the use of load transfer at pavement joints, nonerodible base materials, good drainage practices, and consideration of climatic conditions can lead to pavements that will perform well during the design life.

Channeling is defined as the localized erosion of base, subbase, or subgrade materials caused by flowing water. To occur, it is necessary to have a concentration of water great enough to produce the necessary flow, an erodible material, and sufficient velocity of flow to cause erosion. In contrast, pumping occurs when the pore-water pressure buildup induced by heavy wheel loads is high enough to cause the ejection of material and water through cracks and joints in a pavement slab.

The presence of erodible material and water in the base, subbase, or subgrade hastens the pumping process and leads to loss of foundation support. Recent research work by Phu and Ray (1) and by Dempsey, Carpenter, and Darter (2) indicates that the velocity of water ejected through channels, cracks, and joints can be high enough to cause disintegration, erosion, and subsequent pumping of stabilized bases in addition to unbound bases in rigid pavements.

Large deflections caused by excessive moisture content in the support materials beneath the slab are major problems that affect rigid pavement performance. All failures in the rigid pavement sections at the AASHO Road Test were preceded by pumping of material from beneath the concrete slab (3). Both Yoder (4) and Cedergren (5) noted damage to airport runways and taxiways caused by pumping. These observations were especially prevalent where pavement overload and channelized traffic had occurred. The major forms of distress modes in rigid pavements associated with pumping have been identified by many investigators as faulting (6-10), corner breaking (10-12), transverse and diagonal cracking (10,13,14), and edge punchout (10,15). Additional discussions of pumping and water-related distresses in pavement systems can be found elsewhere (16-19).

OBJECTIVES

This study was conducted to evaluate the mechanisms of channeling and pumping in pavement systems by using laboratory and field investigative procedures. The specific objectives of this study were as follows:

1. Evaluate pumping and channeling in the laboratory by use of a model pavement section,
2. Evaluate pumping and channeling under flexible and rigid pavement sections on the University of Illinois test track facility, and
3. Conduct field investigations of pumping and channeling.

LABORATORY MODEL INVESTIGATION

General

A laboratory study of the mechanisms and results of channeling and pumping in a model pavement system subjected to periodic short-duration loading was completed. Load-induced pore-water pressures in the pavement system were examined with respect to both time and position in the pavement. The study was conducted on a pavement model composed of a subgrade, crushed-limestone base, and portland cement concrete (PCC) surface with an asphalt-concrete shoulder. Channeling and pumping were investigated for three test series by using different gradations of crushed limestone as the base-course material.

Equipment Development

In order to measure the dynamic pore-water pressures in the pavement model, it was necessary to develop a piezometer that could indicate the change in pressure at the instant that loading was initiated. Conventional piezometers that employed porous stones or similar devices were not adequate because of clogging by the fine-grained materials of the base and slow response time. Piezometers that utilized membranes gave erroneous results because of the effective soil pressures against the membrane at the instant of loading. After several pilot studies, the piezometer shown in Figure 1 was developed. It consisted of a small hollow sphere the two halves of which fit snugly together. Small holes about 1 mm (0.04 in) in diameter were placed in the outer half of the sphere. The inner half of the sphere was connected to a small stainless steel tube that was in turn connected to a pressure transducer. A thin rubber membrane was stretched between the two sphere halves before they were sealed together. The inner spherical half and the tube to the pressure transducer were then filled with water to transmit the pressure impulses to the transducer. When the piezometer is placed in a saturated soil or granular material, the effective stress generated by the load is resisted by the sphere, whereas the pore-water pressure can be transmitted through the small holes to the membrane.

Preliminary tests showed that the piezometer functioned well for pore-water pressures that ranged from 0 to 138 kPa (0-20 psi) and pressure durations of 0.1-1.0 s. Pressure tests between a conventional piezometer and the designed piezometer showed excellent correlations. However, the conventional piezometer became plugged with fine material after only a few hundred load applications, whereas the designed piezometer remained unplugged and operational after 20 000 load applications.

base material during repeated loading, a transparent Plexiglas tank 117 cm (46 in) long, 30.5 cm (12 in) wide, and 89 cm (35 in) deep was constructed. Holes were drilled through the side of the tank for installation of the piezometers. The piezometers were extended to the center of the tank about 12.7 cm (5 in) from the inner face so that boundary conditions could be kept to a minimum.

Figure 1. Piezometer for measuring dynamic pore-water pressure.

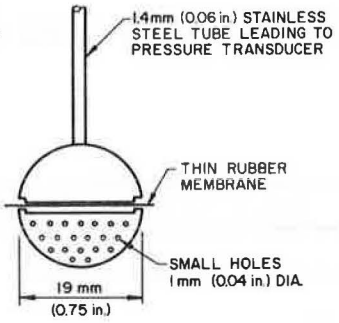

Figure 2. Profile of pavement model.

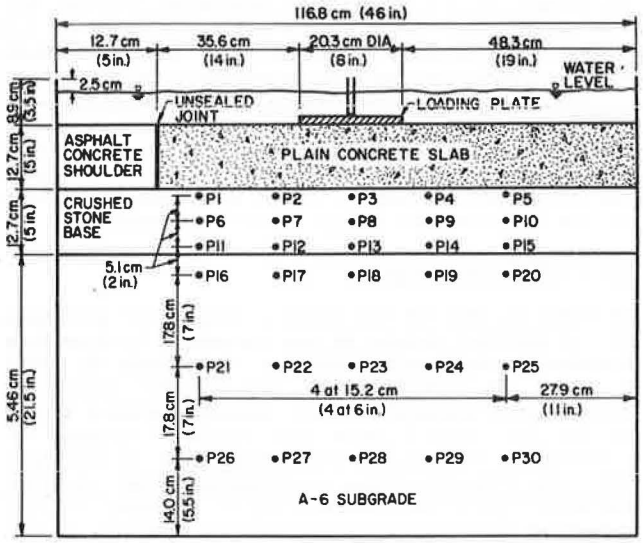

Pavement Model

Figure 2 shows a profile view of the pavement model as placed in the Plexiglas tank. An AASHTO A-6 soil was used as the subgrade material for the pavement model. The subgrade was compacted into the tank in 10.2-cm (4-in) lifts at an average dry density of 1882 kg/m³ (117.5 pcf) and water content of 14.8 percent based on AASHTO T-99. The maximum dry density of the soil was 1698 kg/m³ (106 pcf) and optimum moisture content was 14 percent. Piezometers were placed in the subgrade at the locations shown in Figure 2.

Three pavement model tests were conducted by using three different crushed-limestone gradations as the base course. In test order, the base courses consisted of Illinois CA-7, CA-6, and CA-9 gradations. Table 1 shows the gradation specifications for the different base-course materials. Table 2 shows the gradations and Figure 3 shows the gradation curves for the materials actually used in the model tests. The saturated hydraulic conductivity (coefficient of permeability) for the three aggregate base-course gradations is shown below (1 cm/s = 0.3 ft/day):

Aggregate Gradation No.	Saturated Hydraulic Conductivity (cm/s)
CA-6	2.1×10^{-4}
CA-7	202.0×10^{-3}
CA-9	80.0×10^{-4}

Table 1. Illinois specifications for aggregate gradations.

Gradation No.	Sieve Size (% passing) 37.5 mm	25 mm	19 mm	12.5 mm	9.5 mm	4.75 mm	1.18 mm	300 µm	75 µm
CA-6	100	95±5	–	75±15	–	45±10	25±15	–	8±4
CA-7	100	95±5	–	45±15	–	5±5	–	–	6±6
CA-9	100	97±3	–	60±15	–	30±15	10±10	–	–

Note: 1 mm = 0.04 in.

Table 2. Initial aggregate gradation and that at center of load after testing.

Gradation No.	Sieve Size (% passing) 37.5 mm	25 mm	19 mm	12.5 mm	9.5 mm	4.75 mm	1.18 mm	300 µm	75 µm
Initial Gradation									
CA-7	100	98.1	89.0	64.0	29.9	4.4	0.0	0.0	0.0
CA-9	100	97.5	94.4	65.5	51.5	30.0	11.5	2.1	0.6
CA-6	100	93.0	82.5	73.5	59.7	43.8	30.5	11.3	6.3
Gradation at Center of Load After Testing									
CA-7[a]	100	98.1	89.0	64.0	29.9	4.4	0.0	0.0	0.0
CA-9	100	95.6	88.2	59.7	48.4	31.3	13.8	3.3	0.6
CA-6	100	97.3	86.4	72.3	57.4	42.4	18.2	7.0	2.4

Note: 1 mm = 0.04 in.

[a] Actual gradation of CA-7 was not determined but judged to be the same as prior to testing.

Figure 3. Gradation curves for base courses used in model tests.

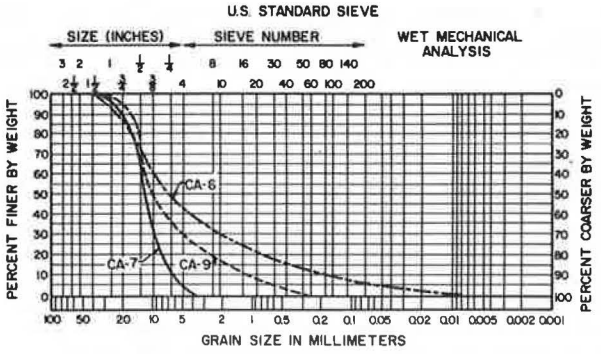

As shown in Figure 2, each base course was constructed to a thickness of 12.7 cm (5 in) and instrumented with piezometers at locations P1 and P15. The subgrade was not replaced during the series of base-course tests. The base course was completely saturated before placement of the concrete surface.

A 12.7-cm (5-in) plain PCC slab was cast in place on the base for each of the three test series and allowed to cure at least seven days prior to loading tests.

An asphalt concrete shoulder section 12.7 cm thick was placed next to the concrete slab as shown in Figure 2. The joint between the concrete slab and asphalt concrete shoulder was not sealed. The concrete slab was loaded through a steel plate 20.3 cm (8 in) in diameter placed 35.6 cm (14 in) from the joint between the shoulder and concrete slab.

Testing Procedure

The testing procedure was developed to determine the pore pressure in the saturated base material and to

Figure 4. Pavement model prepared for dynamic testing.

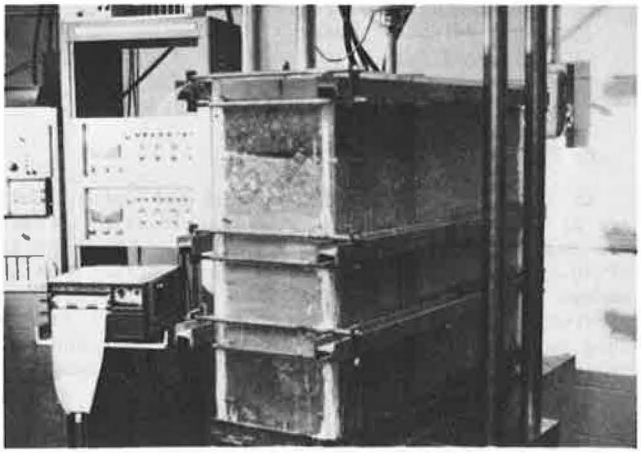

evaluate channeling and pumping caused by repeated loads. Figure 4 shows the pavement model prepared for dynamic testing. The piezometer system was connected to a multichannel recorder. The surface of the pavement was covered with water to ensure that the granular base course and subgrade remained saturated during the test.

The pavement section was loaded so that each pulse exerted by the 20.3-cm-diameter plate remained constant regardless of the slab deformation. The load was increased from 137.9 kPa (20 psi) to 551.5 kPa (80 psi) in 137.9-kPa increments to provide four pressure levels. Each pressure level was maintained for 1 h with 4 s between loads and a load duration of 0.1 s. After testing at the 0.1-s duration, the duration was increased to 1.0 s and the slab was loaded for 5 min at each of the pressure levels. After initial testing, the pavement model was dynamically loaded at one of the pressure levels for 24 h with 4 s between loads and a load duration of 0.1 s. The piezometer readings were monitored at different time intervals during each test period. A tracer dye was injected into the base course at various times so that flow paths and channels could be traced.

After each pavement model had been tested with dynamic loading, the concrete slab and asphalt shoulder were removed and the base course was examined. Base-course samples were obtained at different locations in the pavement model and a gradation analysis was conducted.

Analysis and Discussion of Model Study Results

Several piezometers were placed in the subgrade in order to record the change in pore-water pressure during loading. However, because of the high density and low permeability of the A-6 subgrade, complete saturation was not achieved and the changes in pore pressure were not recorded.

The first gradation of base material tested was CA-7. As determined from Tables 2 and 3 and Figure 3, CA-7 would be considered a coarse-graded material with reasonably high permeability.

In the CA-7 base, it was found that the pore pressures generally decreased with distance and depth from the load. It was found that at no time and at no point in the base did the change in pore pressure exceed 2.1 kPa (0.3 psi). No specific paths of water movement were determined except for the fact that the water near the sides of the test tank and near the concrete slab and asphalt shoulder joint was forced to the surface during loading. It was also found that different load durations of 0.1 s or 1.0 s had little effect on the excess pore pressure in CA-7.

The CA-6 base-course test provided different results than the CA-7 base course, and pore-pressure changes in excess of 20.7 kPa (3 psi) were observed during loading. Table 2 and Figure 3 show CA-6 to be a dense-graded aggregate with a low permeability. The variations in pore pressure were extremely erratic with position in the base course and no pattern could be discerned. However, separate and distinct flow paths were seen in this base-course material, as shown in Figure 5. It appeared that small air bubbles trapped between the particles during saturation would rise to the surface during loading and create a path that water, carrying soil particles, would follow. Large amounts of fine-grained material, most of which passed the 75-μm (No. 200) sieve, were pumped along the sides of the slab (joint between tank wall and slab) and through the joint between the slab and the shoulder to the surface of the slab.

The pore-water pressure results from the test by using the CA-9 base-course material were similar to those from using the CA-6 material and peaked at about 20.7 kPa. As seen in Table 2 and Figure 3, CA-9 has an intermediate gradation between the CA-7 and CA-6 material. CA-9 is not considered to be a highly permeable material, as has been shown above. Figure 6 shows some of the fine material from CA-9 being moved toward the bottom of the joint between the concrete slab and asphalt-concrete shoulder. As found with the CA-7 base course, load durations of 0.1 or 1.0 s had little effect on the excess pore pressures in the CA-6 and CA-9 base courses.

Figure 7 shows the excess pore-water pressure at several positions in the CA-6 base course as the load is increased from 0 to 551.5 kPa (0-80 psi) (see Figure 2 for piezometer locations). The general trend was an increase in pore pressure as the load increased and a diminishing rate of increase as the load became larger. The highest pore pressure occurred directly below the loading plate. The somewhat erratic changes in pore pressure recorded at P2, P12, and P14 may be caused by instrumentation error or by changes in the base-course material during the loading sequence. It was found during testing that the pore pressures would increase uniformly with load as long as the local aggregate structure remained unchanged.

Figure 8 (top) shows more clearly the influence of number of load applications at various stress levels on pore-water pressures in CA-6 and CA-9 base courses. The top diagram in Figure 8 shows a general trend for the pore pressure to increase as the number of loads increases; the bottom diagram shows more erratic pore-water pressure changes with load applications on the CA-6 and CA-9 materials. The fact that the pore-water pressures vary considerably with position in the base may indicate that channels are created that allow passage of water and the transfer of fine materials as noted in Figures 5 and 6.

It would appear that the magnitude of pore-water pressure is an important factor affecting degradation, channeling, and pumping in granular base-course materials. No pumping or degradation was observed in the CA-7 base course, in which the pore-water pressures never exceeded 2.1 kPa. However, the base courses composed of CA-6 and CA-9 experienced pore-water pressures greater than 20.7 kPa and displayed pumping and degradation problems.

According to Phu and Ray (1), aggregate degradation and pumping can be expected in unbound base courses when the water velocity exceeds 5 m/s (16.4 ft/s). In pavements the ejected water velocity can

be estimated from the following energy equation:

$$Z_p + (V_p^2/2g) + (P_p/\gamma_w) = Z_0 + (V_0^2/2g) + (P_0/\gamma_w) + h_f \quad (1)$$

where

Z_p = distance from datum to location in base,
V_p = water velocity in base,
g = acceleration of gravity,
P_p = pore-water pressure in base,
γ_w = unit weight of water,
Z_0 = distance from datum to pavement surface,
V_0 = water velocity at pavement surface,
P_0 = pore-water pressure at pavement surface, and
h_f = friction losses.

If it is assumed that the datum and water level are at the pavement surface and that friction losses are negligible, solution of Equation 1 for a depth of 30.5 cm (12 in) below the pavement surface and an excess pore pressure of 20.7 kPa would indicate an ejected water velocity of about 6.4 m/s (21.1 ft/s). This value exceeds that established by Phu and Ray (1) for degradation and pumping. A similar computation for the CA-7 base course by using an excess pore-water pressure of 2.1 kPa gives a velocity of 2.0 m/s (6.7 ft/s), which is below the criteria of Phu and Ray (1).

The buildup of excess pore-water pressures in the CA-6 and CA-9 base materials was a major cause and/or result of pumping, degradation of the aggregate, and deformation of the concrete slab. There was no appreciable pore-water pressure buildup in the open-graded CA-7 aggregate and there was no observed pumping or aggregate degradation. However, there was considerable slab deformation on the CA-7 base course. Inspection of the CA-7 base material after testing showed that substantial amounts of A-6 subgrade material had intruded into the lower portion of the base course. Subgrade intrusion was not found to be a problem in the CA-6 and CA-9 base-course materials and permanent deformation of the slabs on these materials was actually less than that on the CA-7. However, examination of the changes in gradation of these base-course materials before and after testing showed trends that indicated channeling, degradation, and pumping.

Figure 5. Flow paths of water in CA-6 base course.

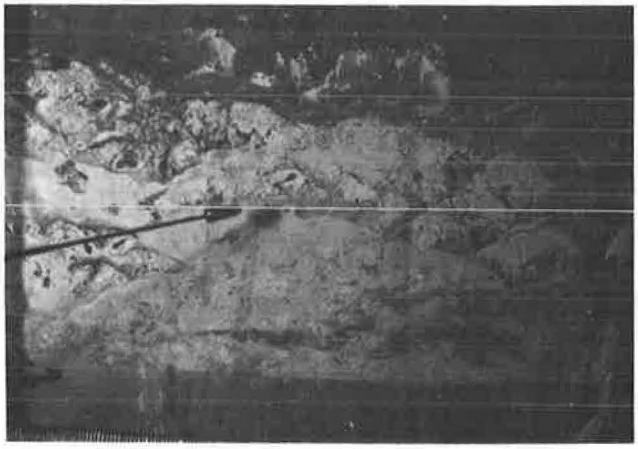

Figure 6. Fine material moving toward concrete slab and asphalt concrete shoulder joint in CA-9 base course.

Figure 7. Influence of applied load on excess pore-water pressure in CA-6 base course.

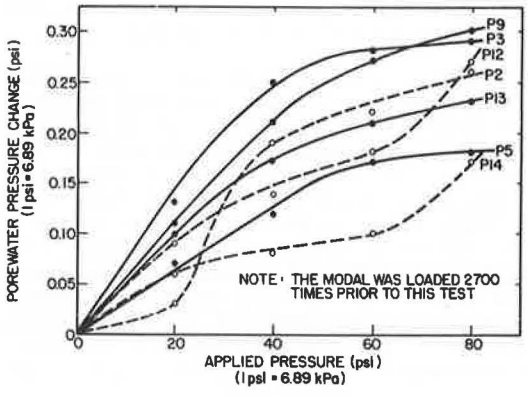

Figure 8. Influence of number of load applications on excess pore-water pressure.

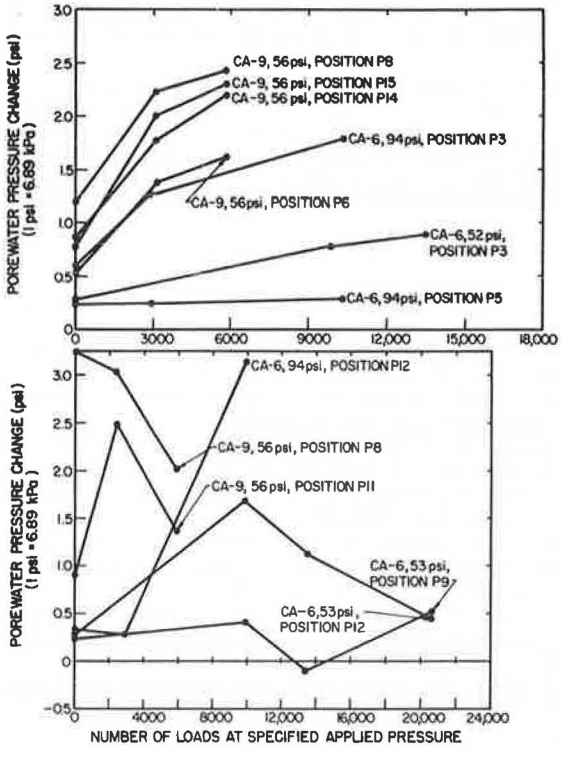

Figure 9. CA-6 base-course gradation changes along interface between concrete slab and base course.

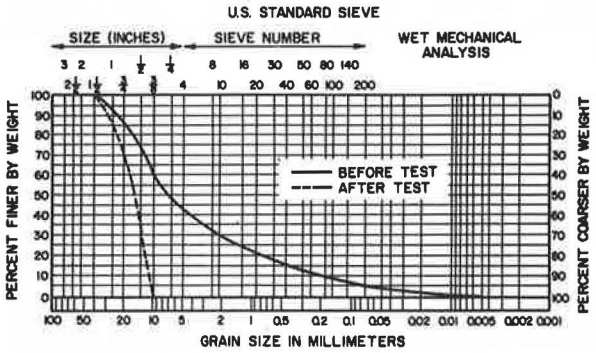

Figure 10. CA-6 gradation changes directly beneath load.

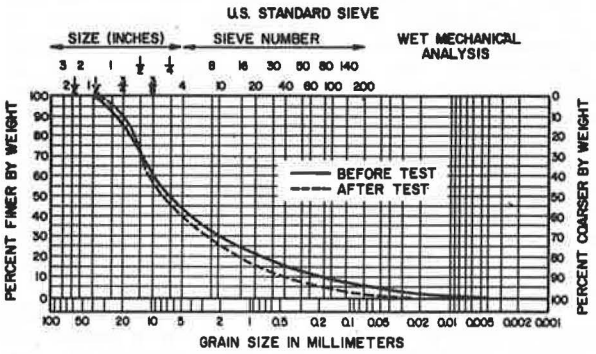

Figure 11. CA-6 base-course gradation changes at joint between concrete slab and asphalt concrete shoulder.

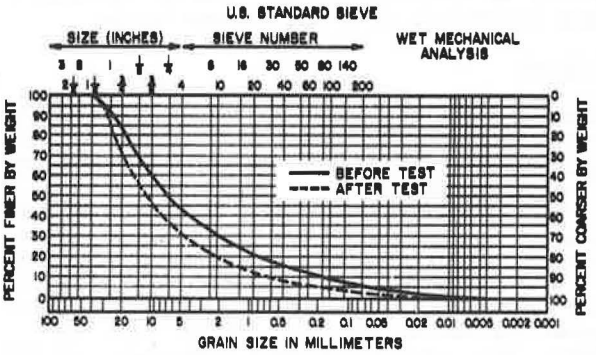

Figure 12. CA-9 base-course gradation changes along interface between concrete slab and base course.

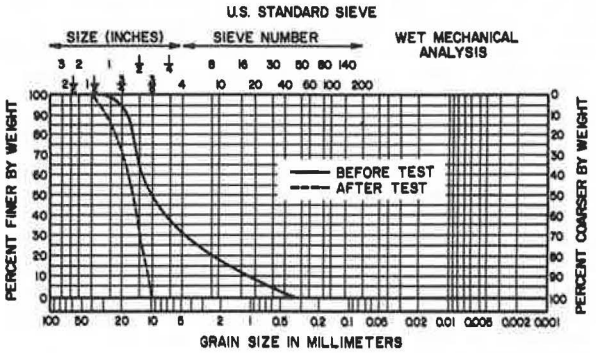

Figure 13. CA-9 base-course gradation changes directly beneath load.

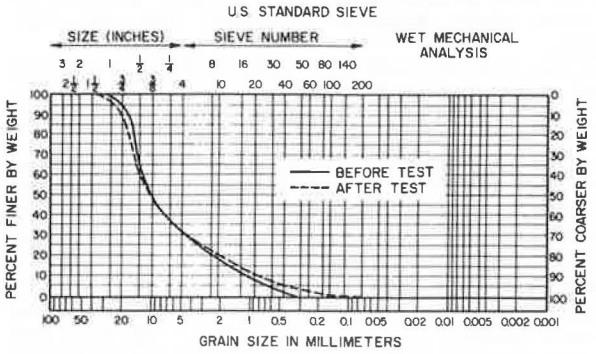

Figure 14. CA-9 base-course gradation changes at joint between concrete slab and asphalt concrete shoulder.

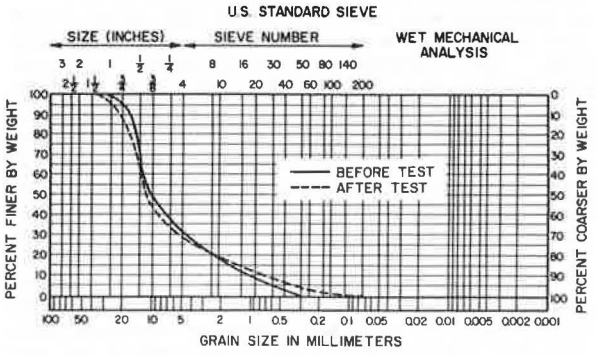

Table 2 shows the base-course gradations before testing and beneath the center of the load after testing. All aggregate gradations used were within the limits of the Illinois Standard Specifications (Table 1) prior to testing.

Figures 9-11 show before and after testing results at various locations in the CA-6 base-course material used in the pavement model. Figure 9 indicates that considerable change in gradation occurred at the interface between the concrete base and the base course (piezometers P1, P2, P3, P4, and P5, Figure 2) during repeated loading. The relative change in gradation indicates that most of the material passing the 10-mm (3/8-in) sieve size was displaced or pumped from directly beneath the slab. Figure 10 shows CA-6 base-course gradation changes beneath the load (piezometers P3, P8, and P13, Figure 2). In general there was some decrease in the percentage of fine material passing the 4.75-mm (No. 4) sieve. The gradation changes in Figure 10 would indicate some displacement and pumping of fine base-course material. Figure 11 shows relative base-course gradation changes directly beneath the joint between the concrete slab and asphalt-concrete shoulder. It is noted that the percentage of base-course material less than 10 mm has decreased substantially. Visual inspection of the base course also indicated that a considerable amount of fine material had been pumped or displaced. Some of the fine material along the top of the base course was found to migrate toward the bottom of the base. Also, large accumulations of base-course fines were found on the surface of the concrete slab and shoulder at the conclusion of testing.

Figures 12-14 show the relative gradations for the CA-9 base-course material before and after testing. Figure 12 shows that substantial gradation change occurred directly beneath the concrete slab

(piezometers P1, P2, P3, P4, and P5, Figure 2) similar to that shown in Figure 9. It is hypothesized that the fine material migrated toward the bottom of the base course or was pumped out. The decrease in percentage of larger material would indicate that some degree of degradation may have occurred. As with the CA-6 material, the CA-9 material passing the 10-mm sieve was displaced or pumped. There was not a large amount of change in the base-course gradations directly under the load (Figure 13) or under the joint between the pavement edge and the shoulder (Figure 14). However, there was an increase in the material smaller than about 2 mm (0.08 in), which would indicate that some degradation had occurred. Substantial fine material was also observed on the surface of the pavement slab and shoulder at the completion of the test.

Inspection of the CA-7 base-course material showed that there were no major gradation changes resulting from repeated loadings. No gradation sampling was accomplished in the lower portion of the base where subgrade intrusion had occurred, however.

In the testing program, the CA-9 base course was tested under 15 000 load applications, whereas the CA-6 base course was tested under 35 000 load applications. The difference in the number of loads resulted from mechanical difficulties during testing of the CA-9 material. Also, there is no doubt that some of the differences in the base-course gradations before and after testing were caused by testing errors and material variability.

Although there are probably some gradation differences resulting from the testing methods, there are some notable trends in the data. In both the CA-6 and the CA-9 base courses, the materials larger than the 10-mm sieve size did not degrade and pump, whereas those smaller did experience degradation and pumping. This is substantiated in the test with the CA-7 base material in which approximately 95 percent of the material was retained above the 10-mm sieve size and no pumping or appreciable gradation changes occurred. The largest gradation change occurred directly beneath the slab on the base-course surface followed by change in gradation below the shoulder. A smaller gradation change is noted as samples are taken deeper into the base course beneath the load or below the shoulder. In the pumping observations, water and soil directly beneath the slab were forcefully pumped up along the joint between the slab and tank wall and up through the joint between the slab and the shoulder. The major flow path in the model appeared to be toward the shoulder and up through the joint; less material was moved as distance from the shoulder increased. Visual inspections of the model during loading revealed that, as the number of loads increased, water turbulence became more evident under the slab and near the shoulder. Even though a clear and concise distribution of excess pore pressures could not always be recorded, it was found that the maximum pressures developed near the base of the slab and near the shoulder (along the path of pumping).

The development of flow channels was observed in the granular base materials. Although these channels provided for water movement and therefore the dissipation of pore-water pressures during loading, they also provided a pathway for the movement of fine materials. Since the channels contribute to the displacement and pumping of fine base and subgrade materials, they are probably not an asset to pavement performance.

Examination of the permeabilities of the base materials helps to explain why the CA-6 and CA-9 base courses developed higher excess pore pressures then the CA-7 base course did. Table 2 shows that CA-7 is much more permeable than CA-6 and CA-9. Consequently, the dissipation of excessive pore pressures was extremely rapid in CA-7, and the base course did not experience water channeling or pumping.

TEST TRACK INVESTIGATION

General

As a bridge between laboratory testing and full-scale road tests, the testing of prototype pavement sections in a traffic-simulating testing operation can sometimes provide much information. Because the prototype sections are nearly full scale, tests performed on the test pavement provide information indicative of field behavior. Since close control of construction, climate, and traffic loading is possible, the performance of the pavement and the effect of the variables can be determined.

Ahlberg and Barenberg (20) have reported on the use of the University of Illinois test track to model pavement systems and evaluate pavement design and performance. The test track has been found to provide a flexible method for evaluating the influence of water and drainage on pavement performance.

In an agreement between the University of Illinois and the New Jersey Department of Transportation (NJDOT), the test track was used to conduct a study entitled Evaluation of Drainage Systems for Pavements. This study, under the supervision of Barenberg, was concerned with the evaluation of open-graded bases under flexible and rigid pavements.

As part of the study to evaluate channeling and pumping, a request was made to analyze a number of New Jersey pavement sections being tested at the Illinois test track.

The specific objectives of the study were to measure and evaluate the saturated hydraulic conductivity of open-graded bases and to investigate pumping and channeling in the pavement system.

Test Track

A schematic diagram of the University of Illinois test track is shown in Figure 15. A more thorough discussion of the geometrics of the test track can be found elsewhere (20).

Construction of the test sections and the transition zones between them is done at a scale similar to that of actual pavements. This procedure allows for more uniform control and better simulation of actual pavement construction. Mixing equipment prepares batches of material 136 kg (300 lb) or greater. The material is then distributed in the appropriate section and leveling frames trim the material to the desired thickness in each section. Compaction is done with small maintenance equipment such as vibratory plate compactors, vibratory rollers, or mechanical impact compactors.

Pavement Test Sections

Six asphalt pavement sections were tested in the first phase and four PCC pavement sections were tested during the second phase. The six asphalt concrete and four PCC pavement sections are described in Table 3. The original design thicknesses are scaled down so that the 1451-kg (3200-lb) single-wheel load [551.5 kPa (80 psi) tire pressure] used in the test track induces a similar stress-strain response as would occur with a 4082-kg (9000-lb) dual-wheel load.

A special feature of the drainage layer study was the need to test the hydraulic capabilities of the test sections. To facilitate these measurements,

plastic sheeting was placed on each side of the cross section from the silty-clay (AASHTO A-6) subgrade to the base-course material and extended from the inner to outer pit wall. Next to the inner curb, each section was provided with an inflow trench so that water could be input uniformly into the layer immediately beneath the drainage material. For the sections with open-graded drainage layers, water was confined by impermeable surfaces so that it flowed into the drainage layer a distance of 30.5 cm (1 ft), after which it could then flow as it would in the field (section had a 1 percent transverse slope). An outflow trench was constructed next to the outer curb for each of the pavement sections.

Figure 15. Schematic diagram of University of Illinois pavement test track.

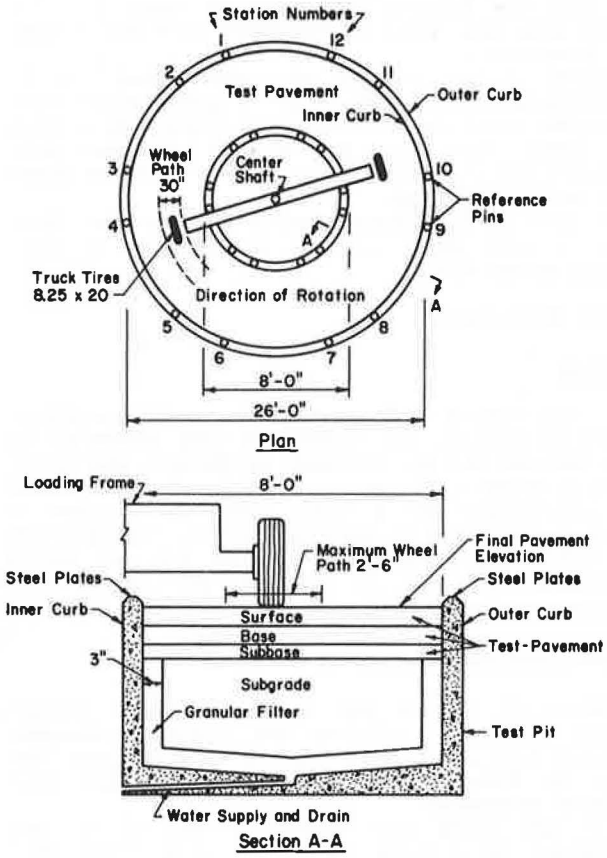

Table 3. Description of test sections used in test track.

Section	Layer Thickness (in) Section No. 1	2	3	4	5	6
Phase 1: Asphalt Concrete Pavement Sections						
Medium aggregate bituminous concrete	2	2	2	2	1.5	2
Bituminous stabilized base course	3	3	3	3	2	3
Bituminous stabilized open-graded layer	–	2.5	2.5	–	2.5	2.5
Nonstabilized open-graded layer	–	–	–	2.5	–	–
Lime-fly ash stabilized (5A)	–	–	–	2	2	–
Lime-fly ash stabilized sand-gravel mixture	–	–	–	–	–	3
Well-graded crushed-stone base (5A)	4	4	4	2.5	2.5	–
Well-graded silty gravel (1B)	8	5	5	5	5	6
Phase 2: Portland Cement Concrete Pavement Sections						
PCC	3	3	3	3	–	–
Nonstabilized open-graded	2	–	3	3	–	–
Lime-fly ash stabilized (1C)	2.5	–	–	–	–	–
1C with 5 percent clay fines	–	3	–	–	–	–
1C with 8 percent clay fines	2.5	4	4	4	–	–
Filter cloth (Bidim)	No	No	No	Yes	–	–

Note: 1 in = 25 mm.

Test Results and Discussion

The drainage layers evaluated in the six asphalt-concrete pavement sections consisted of a bituminous stabilized open-graded (BSOG) layer, nonstabilized open-graded (NSOG) layer, and a well-graded crushed-stone base (5A) (Table 3). Small piezometric tubes were placed at various locations in the drainage layers in different segments of the test track for the purpose of measuring the hydraulic heads necessary for determining the saturated hydraulic conductivity.

BSOG was found to have an average saturated hydraulic conductivity of 1.8 cm/s (5100 ft/day) at the end of the test. NSOG had a slightly higher conductivity of 1.9 cm/s (5386 ft/day). The well-graded crushed-stone base (5A) had an average conductivity of 5.2×10^{-3} cm/s (15 ft/day). [It was noted that in some locations the 5A base had a conductivity less than 3.5×10^{-4} cm/s (1 ft/day).]

Evaluation of the pavement sections based on rutting and roughness indicated that the NSOG layer gave the best performance. The BSOG layer performance was evaluated to be slightly below that for NSOG. As expected, the crushed-stone base (5A) displayed poor performance. There was no indication of pumping in any of the test sections and there was no indication of channeling in the drainage layers when the pavement sections were excavated after completion of the test.

In the PCC pavement sections (Table 3), the NSOG material was prepared by blending two aggregates (57 and 9, supplied by NJDOT) on a 50-50 basis. The final gradation of this material is given below (1 mm = 0.04 in):

Sieve Size	Percent Passing
25 mm	98
19 mm	78
12.5 mm	62
9.5 mm	53
4.75 μm	35
2.36 μm	5
425 μm	0.5

The subbase material 1C (Table 3) was a blend of pit-run gravel, river sand, and silt proportioned to meet the requirements of the 1C material as specified by NJDOT. A gradation of this material along with the laboratory and in situ densities and the measured saturated hydraulic conductivities at two different densities are as follows (1 pcf = 16 kg/m³; 1 ft/day = 3.5×10^{-4} cm/s):

1. Sieve size and percent passing: 19 mm, 91; 4.75 mm, 76; 300 μm, 13; 150 μm, 9; 75 μm, 8;
2. Compaction moisture content, 5.5 percent: dry in-place density (avg), 120 pcf; dry maximum density T-99, 129 pcf; and
3. Permeability: 135 pcf, 1.2 ft/day; 129 pcf, 1.8 ft/day; 120 pcf, none.

The permeability of the NSOG material was measured under a vertical head and found to vary from approximately 0.9 to 1.8 cm/s (2500-5100 ft/day) with densities from around 1762 to 1842 kg/m³ (110-115 pcf). The mean value for the permeability of the NSOG materials was determined to be 1.2 cm/s (3400 ft/day) with an average density of 1810

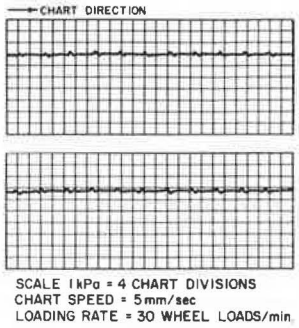

Figure 16. Dynamic pore-water pressure for section 4.

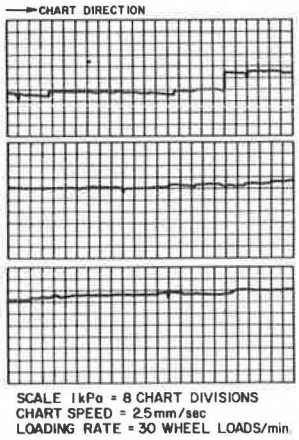

Figure 17. Residual pore-water pressure for transition section with 1C material and 8 percent clay.

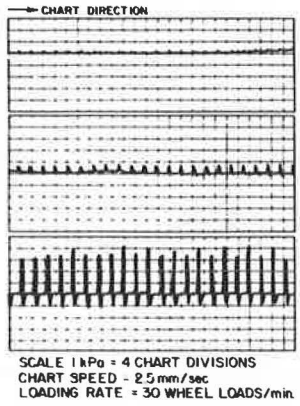

Figure 18. Dynamic pore-water pressure for transition section with 1C material and 8 percent clay.

kg/m³ (113 pcf). Through use of the dynamic piezometer shown in Figure 1, the residual and dynamic pore-water pressures were measured at the bottom of the PCC slab in sections 2 and 4 and at a transition section composed of 19.1 cm (7.5 in) of 1C material with 8 percent clay. The piezometers were placed next to the wheel path.

Figure 16 shows the dynamic pore-water pressure for section 4 in which the NSOG material was used. Figures 17 and 18 show residual and dynamic pore-water pressures, respectively, in a dense-graded aggregate transition section. Section 2 was already pumping when the pore-water pressure measurements were started and showed pressure responses similar to those in Figure 18. Pore-water pressures in sections 1 and 3 were not tested.

Figure 16 shows that the dynamic pore-water pressure developed in the saturated NSOG material was only about 0.5 kPa (0.07 psi). There was no residual pore-water pressure development noted in the NSOG material.

In Figure 17 the residual pore-water pressure development in the dense gravel material was about 2.2 kPa (0.32 psi). With the low confining pressures, σ_3, found in this pavement system, the pressure is probably adequate to start liquifaction of the base-course material. Figure 18 shows dynamic pore-water pressures in the dense gravel once pumping and channeling have started. The maximum saturated pore-water pressure is about 5 kPa (0.72 psi). A pressure of 5 kPa would convert to a pumping head of about 51 cm (1.7 ft). It is interesting to note the negative pressures of about 1.2 kPa (0.17 psi) that occur as the wheel load passes over the piezometer.

Based on the limited test track study, it is hypothesized that loads on dense-graded base-course materials first cause residual pore-pressure buildup and liquifaction, which are followed by dynamic pore pressure and pumping once the channel for the pressure outlet is formed.

A more thorough discussion of the data and findings of this study will be published in a final report to the NJDOT.

FIELD INVESTIGATION

General

Both qualitative and quantitative field investigations of pumping and channeling were conducted in the FHWA project on improving subdrainage and shoulders of existing pavements. Pumping was found to be distinguishable and a major cause of distress in concrete pavements in numerous states. The evidence of channeling in pavement systems was not easily determined and not as apparent as pumping when distress mechanisms are evaluated.

Field Investigation Results

Evidence of pumping and loss of material beneath concrete pavement sections was found in climates ranging from semiarid to wet. It was apparent that both the frequency and magnitude of rainfall were related to pumping.

It was found that pavements located on long gradients in rolling topography were often most vulnerable to pumping and bleeding of water and fines from the support materials. Figure 19 shows water and fine material flowing out from beneath a jointed concrete pavement system located on a long gradient. It is probable that water channeling also exists in this pavement system. In some areas with rolling topography, pavement cuts through the top of a hill will often intercept groundwater sources, which will cause water flow along the pavement profile. This condition is easily recognized by the growth of cattails or other water plants in the ditches at the crest of the hill.

Figure 20 shows that pumping can be associated with continuously reinforced pavement systems as well as with jointed pavement systems when the distress state becomes severe. Furthermore, surveys of pavements in Illinois showed evidence of disintegration and pumping in subbases composed of cement aggregate mixtures (CAM) and bituminous aggregate mixtures (BAM). Figure 21 shows disintegrated BAM that has been pumped out from beneath a section of continuously reinforced concrete pavement.

Figure 22 displays a cement-treated subbase after the concrete pavement slab has been removed (from Woodstrom of the California Department of Transportation). The channeling that has occurred at the interface between the slab and cement-treated sub-

base can be noted by the light areas formed by grout injection.

Figure 23 shows a section of pavement being prepared for a patch. Even though there was a longitudinal subdrain next to the pavement edge, the water did not freely drain from the pavement section. Even after several hours, water was still visible next to the pavement edge. Inspection of the pavement section indicated that fine material was responsible for blocking the flow of water to the longitudinal subdrainage trench.

Field investigations generally showed that water-related distresses in the mainline pavement also extended to the shoulder. Shoulder drop-off resulting from the ejection of base course or subgrade fines from beneath the shoulder and disintegration and erosion of the shoulder material along the joint between pavement and shoulder were evident in numerous pavement systems inspected. These joint openings would often be more than 2.5 cm (1 in) wide, and water could frequently be seen in the joint.

Field investigations and drainage studies by Dempsey and Robnett (21) have indicated that the joint between pavement and shoulder contributes to most of the water infiltration into a pavement system. Subdrainage outflow studies on pavement test sections in Georgia and Illinois indicated that water infiltration into the pavement section could be substantially reduced by edge sealing. Table 4 shows outflows measured at the two test sites and indicates the differences in infiltration volume for

Figure 19. Water and fine material flowing out from beneath jointed concrete pavement on long gradient.

Figure 20. Pumping associated with continuously reinforced concrete pavement.

Figure 21. BAM pumped from beneath continuously reinforced concrete pavement.

Figure 22. Channeling marks at interface between concrete slab and cement-treated base.

Figure 23. Patching continuously reinforced concrete pavement with edge drain.

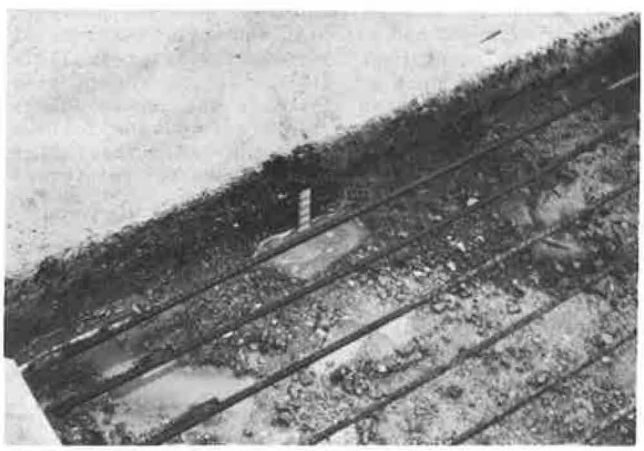

Table 4. Statistical data based on percentage of pipe outflow.

Section	Mean ($\bar{x}$) (%)	Coefficient of Variation (V) (%)	SD (%)
Georgia G1 unsealed	30.6	61.1	18.7
Georgia G1 sealed	0.7	194.0	1.4
Georgia G2 sealed	–	–	–
Illinois I1 unsealed	26.0	76.5	19.9
Illinois I1 sealed	16.4	69.5	11.4
Illinois I2 unsealed	52.1	36.7	19.1
Illinois I2 sealed	11.6	28.4	3.3

Note: Percentage of pipe outflow = [(pipe outflow volume)/(precipitation volume)] x 100.

Figure 24. Effect of loss of pavement edge support on critical stresses and deflections.

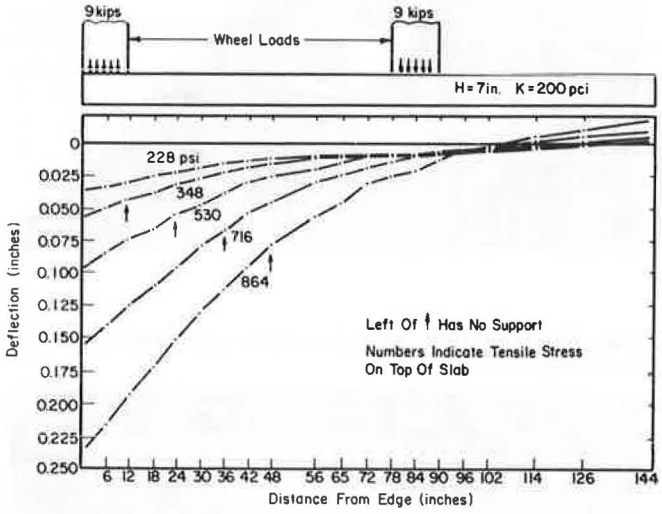

unsealed and sealed edge joint conditions. In the Georgia G2 section, both the transverse and the longitudinal joints were sealed, and no measurable outflow was observed over the duration of the test.

Analysis and Discussion of Field Results

In a National Cooperative Highway Research Program project report, Darter and Snyder (22) studied the distress types and mechanisms of 966 km (600 miles) of jointed reinforced concrete Interstate pavement in Illinois. Of 204 projects surveyed they found 137 that displayed evidence of pumping. Of the 137 projects that displayed pumping, in 20 percent there was high-severity pumping; in 32 percent, medium-severity; and in 48 percent, low-severity.

Although the jointed reinforced concrete pavement sections surveyed had granular subbases, a survey of continuously reinforced concrete pavements in Illinois showed evidence of disintegration and pumping of CAM and BAM subbases (15). In the report summarizing the results of the field survey, the following quote was made concerning the BAM subbase that is predominantly used in continuously reinforced concrete pavement systems (15):

> During the field surveys, numerous edge punchouts were observed as the maintenance crew removed the broken concrete. There was frequently a considerable amount of free moisture within the failure area and the BAM subbase was disintegrated and had been intruded by fine-grained soil.

A major result of pumping is the loss of support under the concrete slab, which can cause high stresses and deflections that then lead to an accelerated rate of distress. Based on pavement stress analysis, Figure 24 (23) shows that, as loss of support increases, the maximum stresses and deflections increase and the point of maximum stress moves in from the edge. For example, as the loss of support moves in 60 cm (2 ft) from the pavement edge, the tensile stress in the slab increases 132 percent and edge deflection increases about 75 percent. This loss of support is responsible for much of the faulting, longitudinal cracking, corner cracking, and punchouts observed in concrete pavement systems.

Laboratory studies and field observations indicate that the pumping mechanisms vary depending on the type of base course used. From laboratory and field studies, it is observed in unbound granular base courses that fine materials are generally displaced throughout the full depth as a result of load-induced pore-water pressures. In stabilized bases such as CAM and BAM, the fine materials are generally removed or eroded from the interface between the concrete slab and stabilized base or stabilized base and subgrade. In both the unbound bases and stabilized bases there can be either intrusion or pumping of the subgrade materials.

In a recent study of problems caused by the presence of water in concrete pavements, Phu and Ray (1) developed relationships for determining the critical water velocity that would cause erosion of the subbase course. They showed the relative water velocities causing erosion in unbound and stabilized subbases subjected to zero and nine freeze-thaw cycles. Phu and Ray (1) indicated that an unbound gravel does not resist the expulsion of water on the order of 5 m/s (16.4 ft/s) and pumping of the fines will occur rather frequently. They indicated that pumping at this water velocity is more severe in pavements without dowels than in those with dowels.

Phu and Ray (1) have found that water velocities ranging from 0.1 to 1 m/s (0.3-3.3 ft/s) were sufficient to displace fines from the top to the bottom of the subbase or from the interior toward the exterior pavement joints. During the study of partial displacement they found that a suction pressure is often produced in the water beneath the concrete slab with passage of load. The development of suction pressures was also found with the passage of load during the test track study phase of this project (Figure 18).

The ejection of water is a function of pressure and it is influenced by the joint opening. In general there is a decrease in the water ejection velocity as the size of the joint opening increases. Important factors causing pumping are slab curling and the development of a cavity beneath the concrete pavement slab. A water-filled cavity of 0.5 mm (0.02 in) or greater can create expulsion water velocities great enough to cause pumping under normal loading conditions. It is for this reason that eroded cavities beneath concrete pavements must be sealed to prevent serious water problems after pavement rehabilitation.

When pumping problems in jointed concrete pavements are evaluated, it is important to understand the influence of slab thickness. Based on work at the Laboratoire Centrale des Ponts et Chaussées (24), the following quotation is presented concerning concrete slab thickness:

> Today, studies based upon the observation of stair-stepping (faulting) and the precise recording of deformations on experimental thick-slab sections have demonstrated qualitatively that the dissymmetry of slab-end deformations was not substantially modified and that an increase in thickness could only change the stair-stepping

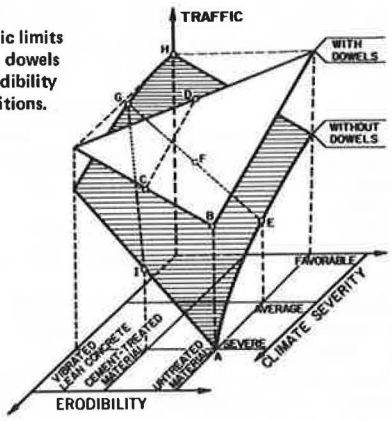

Figure 25. Areas representing traffic limits with and without dowels depending on erodibility and climate conditions.

rate. For example, a 10 percent increase in slab thickness can reduce stair-stepping by only about 25 percent when the subbase is treated.

In current design practice, slab thickness is determined so as to avoid slab fatigue cracking, and not with a view to optimum load transfer at joints. As regards pumping and stair-stepping, they are usually approached in terms of factors other than slab thickness. Further, several countries do not take the existence of dowels directly into account in the practical calculation of motorway slab thicknesses. In fact, if joint behavior is to be sufficiently modified, the cost of increasing the thickness of the concrete slab is such that other arrangements are more effective (less erodible foundation, dowels for example). Structural design studies in different countries moreover confirm this observation. An increase in thickness is considered only when it allows other simplifications, which is the case for example with very thick slabs resting directly on a porous subgrade (4/60 mm particle size, for example).

In order to show the interaction among traffic, climate, subbase materials, and joint load transfer, the laboratory (24) developed the three-dimensional space representation shown in Figure 25 (24). Figure 25 provides a qualitative model for the interactive parameters that need to be considered in pavement design in order to minimize pumping and erosion. Two material properties of great importance to pumping are compressibility and saturated hydraulic conductivity (permeability).

From this research study it is felt that subbases beneath existing pavement systems must be drainable if subdrainage systems are to be effectively used. It is hypothesized that subdrainage systems will have little influence on pore-water pressure buildup and pumping in subbases with K_s < 0.009 cm/s (25 ft/day), some influence for K_s = 0.009-0.09 cm/s (25-255 ft/day), and appreciable influence for K_s > 0.09 cm/s.

It is evident that climatic conditions are important to pavement rehabilitation and design. Field studies indicate that load transfer at the pavement joint will improve pavement performance. It is also apparent that the stability, strength, and drainability of the base-course materials are very important factors influencing the long-term performance of the pavement system.

SUMMARY AND CONCLUSIONS

Summary

Conditions that cause pumping and channeling in pavement systems were studied in the laboratory and field. Laboratory pavement model tests indicated that dense-graded crushed-stone base courses would experience channeling and pumping under dynamic loading conditions. An open-graded crushed-stone base did not pump, but subgrade intrusion caused permanent deformation of the pavement slab.

The University of Illinois test track was used to study six asphalt-concrete pavement systems and four PCC pavement systems. It was found that asphalt-concrete pavements on both NSOG and BSOG layers performed well under repeated wheel load. The pavement on a well-graded crushed-stone base displayed the poorest performance. The PCC pavement slab on an open-graded base course did not pump, whereas that on a dense-graded base course displayed residual and dynamic pore-water pressures that led to pumping.

Field investigations show that pumping continues to be a problem in pavements. However, it is indicated that the use of load transfer at pavement joints, nonerodible base materials, good drainage practices, and consideration of climatic conditions can lead to pavements that will perform well during the design life.

Conclusions

From the research on channeling and pumping the following conclusions are presented:

1. Excess pore pressure, developed as a consequence of loading, will increase as the applied load increases.
2. Excess pore pressure will increase as the number of loads increases.
3. Excess pore pressure will increase as the permeability of the base course decreases and material compressibility increases.
4. Excess pore pressure beneath a pavement system with a fine-grained base material can reach at least 20.7 kPa (3 psi), which is sufficient pressure to pump fine-grained material to the surface.
5. Materials in the base of a pavement system smaller than the 10-mm sieve size are subject to degradation and pumping.
6. Although channeling may aid drainage, it is detrimental from the standpoint of displacement of fine base and subgrade materials and pumping.
7. Climatic conditions must be considered in pavement rehabilitation and design.
8. Load transfer devices at pavement joints can decrease faulting and pumping.
9. Stabilized bases and subbases can improve pavement performance.
10. Stabilized bases and subbases must be designed to resist erosion by water.
11. Stabilized open-graded bases and nonstabilized open-graded bases in combination with a subdrainage system can improve pavement performance.
12. Subgrade intrusion must be considered when open-graded materials are used as subbases.
13. Pavement layer drainability must be considered in the design of subdrainage systems.

ACKNOWLEDGMENT

This paper was prepared from a research study on improving subdrainage and shoulders of existing pavements, which was conducted at the Department of

Civil Engineering, University of Illinois at Urbana-Champaign, under the sponsorship of the Federal Highway Administration, U.S. Department of Transportation. George Ring III of the Federal Highway Administration was the project monitor.

The contents of this paper reflect my views, and I am responsible for the facts and the accuracy of the data presented herein. The contents do not necessarily reflect the official views or policies of the Federal Highway Administration. This paper does not constitute a standard, specification, or regulation.

REFERENCES

1. N.C. Phu and M. Ray. L'Erodabilité des Materiaux de la Couche de Fondation et de la Couche de Forme des Chaussées en Beton. Chaussees en Beton, Laboratoire des Ponts et Chaussées, Paris, 1979.
2. B.J. Dempsey, S.H. Carpenter, and M.I. Darter. Improving Subdrainage and Shoulders of Existing Pavements. FHWA, Final Rept., 1980.
3. The AASHO Road Test: Report 7. HRB, Special Rept. 61G, 1962.
4. E.J. Yoder. Pumping of Highway and Airfield Pavements. Purdue Univ., West Lafayette, IN, Joint Highway Research Project, 1946.
5. H.R. Cedergren. Methodology and Effectiveness of Drainage Systems for Airport Pavements. U.S. Army, Construction Engineering Research Laboratory, Champaign, IL, Tech. Rept. C-13, 1974.
6. W. Gulden. Investigation into the Causes of Pavement Faulting on the Georgia Interstate System. Office of Materials and Tests, Georgia Department of Transportation, Atlanta, Interim Rept. 2, 1974.
7. D.L. Spellman, J.H. Woodstrom, and B.F. Neal. Faulting of Portland Cement Concrete Pavements. Materials and Research Department, State of California, Sacramento, Res. Rept. M&R 635167-2, 1972.
8. R.G. Packard. Design Considerations for Control of Joint Faulting of Undoweled Pavements. Proc., International Conference on Concrete Pavement Design, Purdue Univ., West Lafayette, IN, 1977.
9. J.H. Woodstrom. Improved Base Design for Portland Cement Concrete Pavements. Proc., International Conference on Concrete Pavement Design, Purdue Univ., West Lafayette, IN, 1977.
10. S.H. Carpenter, M.I. Darter, and B.J. Dempsey. A Pavement Moisture Accelerated Distress (MAD) User's Manual. FHWA, 1980, Vol. 2.
11. J.P. Zaniewski. Economic Considerations of Faulting and Cracking in Rigid Pavement Design. TRB, Transportation Research Record 602, 1976, pp. 1-8.
12. E.J. Barenberg, C.L. Bartholomew, and M. Herring. Pavement Distress Identification and Repair. U.S. Army, Construction Engineering Research Laboratory, Champaign, IL, Tech. Rept. P-6, 1973.
13. R.E. Frost. Correcting Pavement Pumping by Mudjacking--Indiana. HRB, Res. Rept. 1-D, 1945, pp. 13-54.
14. C.A. Hogentozler. Report of Investigation of the Economic Value of Reinforcement in Concrete Roads. Proc., HRB, Vol. 6, 1926.
15. S.A. LaCoursiere, M.I. Darter, and S.A. Smiley. Performance of Continuously Reinforced Concrete Pavements in Illinois. FHWA, Rept. FHWA-IL-UI-112, 1978.
16. B.J. Dempsey, M.I. Darter, and S.H. Carpenter. Improving Subdrainage and Shoulders of Existing Pavements--State of the Art. FHWA, Interim Rept., 1980.
17. S.H. Carpenter, M.I. Darter, and B.J. Dempsey. A Pavement Moisture Accelerated Distress (MAD) Identification System. FHWA, 1980, Vol. 1.
18. S.H. Carpenter, M.I. Darter, and B.J. Dempsey. Evaluation of Pavement Systems for Moisture-Accelerated Distress. TRB, Transportation Research Record 705, 1979, pp. 7-13.
19. M. Ray. A European Synthesis on Drainage, Subbase Erodibility, and Load Transfer in Concrete Pavements. Proc., 2nd International Conference on Concrete Pavement Design, Purdue Univ., West Lafayette, IN, 1981.
20. H.L. Ahlberg and E.J. Barenberg. The University of Illinois Pavement Test Track--A Tool for Evaluating Highway Pavements. HRB, Highway Research Record 13, 1963, pp. 1-21.
21. B.J. Dempsey and Q.L. Robnett. Influence of Precipitation, Joints, and Sealing on Pavement Drainage. TRB, Transportation Research Record 705, 1979, pp. 13-23.
22. M.I. Darter and M.B. Snyder. Development of a Nationwide Concrete Pavement Evaluation System. NCHRP, Interim Rept., 1980.
23. M.I. Darter, S.A. LaCoursiere, and S.A. Smiley. Structural Distress Mechanisms in Continuously Reinforced Concrete Pavements. TRB, Transportation Research Record 715, 1979, pp. 1-7.
24. Le Transfer de Charge aux Joints Transversaux de Retrait-Flexion et la Conception des Chaussées en Beton. Chaussées en Beton, Laboratoire Centrale des Ponts et Chaussées, Paris, 1979.

Subbase Permeability and Pavement Performance

GARY L. HOFFMAN

Problems of premature pavement and shoulder distress in Pennsylvania have been attributed to excess water in the standard, dense-graded subbase. An experimental project was constructed to demonstrate the feasibility of providing good support and good internal drainage to the single layer of subbase with a two-layer system at a competitive cost. An additional long-term objective of the project was to determine the significance of the permeability of subbase layer materials on pavement performance. Five types of subbases, ranging from a very impermeable cement-stabilized material to a very permeable and uniformly graded crushed aggregate, were incorporated into the project. The study documented the manufacturing of the various materials and the associated unit costs. Base materials with permeabilities 3 orders of magnitude more than that of the standard subbase were placed for only a 5 percent increase in cost. The ability of the contractor to handle, place, and pave on the various subbases was evaluated. In-place permeabilities were measured with the field permeability test device developed by L.K. Moulton of West Virginia University to statistically determine permeability by variation within a material section and between the five material sections. Initial pavement roughness measurements were made on the concrete pavement in each experimental sec-

tion, and these measurements indicated no loss in construction quality with the use of the more permeable interlayers. Underdrain system outlets were instrumented so the rates at which the various subbase materials carry off infiltrated surface water could be determined throughout the long-term evaluation.

The current Pennsylvania Department of Transportation (PennDOT) specification for crushed-aggregate subbase (PA 2A) was developed over a number of years as a result of extensive testing, evaluation, and field performance monitoring. The gradation specifications were chosen to provide (a) the necessary strength and stability to support construction equipment, the pavement, and subsequent traffic; (b) drainage; and (c) a material that could be manufactured with adequate quality control at reasonable cost. The specification was developed as a compromise that would best meet the above criteria.

Several problems of premature pavement and shoulder distress have been attributed to excess water in the pavement system, and questions have been raised as to the adequacy of the current PA 2A subbase to provide sufficient drainage for the pavement system. Laboratory permeability tests of the 2A subbase indicate a range in the coefficient of permeability of 1×10^{-3} to 1×10^{-5} cm/s. This range of permeability represents a very slow to nearly impermeable material. Field permeability of the subbase is varied because of in situ gradation variations at the same job site and seems to be higher in some cases than indicated by the laboratory tests. Recent field permeability tests conducted as part of a nationwide study by L.K. Moulton and Roger Seals of West Virginia University (1) on PennDOT subbase indicate permeabilities in the range of 10^{-1} to 10^{-2} cm/s.

This experimental construction project was devised to demonstrate the feasibility of providing good support and good internal drainage at a competitive cost to our current subbase. These facts were recently demonstrated in a similar project in Kentucky (2). An additional long-term objective of the project was to determine the significance of the permeability of subbase layer materials on pavement performance. The subbases were to represent a range in permeability from impermeable to very permeable.

The project field site was located on traffic route 66 (Legislative Route 203) in Armstrong County, Pennsylvania. Five sections of base/subbase materials representing a range of permeability conditions from impermeable (aggregate-cement) to very permeable (PA 2B aggregate) were constructed. The standard design was the placement of 25 cm of reinforced concrete pavement (RCP) on 33 cm of PA 2A densely graded aggregate subbase (control section). In the experimental sections, other materials were placed as an interlayer between the PA 2A subbase and the RCP as shown in the pavement cross sections (Figures 1-5). The total thickness of the experimental interlayer and the subbase was 33 cm for all sections. Each experimental section was between 304 and 509 m long and was constructed in adjacent sections in both the northbound and southbound lanes of the four-lane divided highway.

MATERIAL PROPERTIES

Laboratory Testing

Laboratory testing was done to determine the particle size distribution curves, the maximum dry densities, and the corresponding permeabilities of each of the five material types. All aggregate material was a glacial sand and gravel that was shipped from Davison Sand and Gravel's Tarrtown Flats source.

The specified gradation limits for the standard PA 2A gradation, the high-permeability (HP) gradation, and the unstabilized PA 2B gradation are shown in Figure 6. The PA 2A and the HP materials are both well graded, but the HP material has coarser fragments than the PA 2A throughout its entire particle size distribution. The PA 2B gradation band is narrow, and this material is uniformly sized. The actual distribution curve of the unstabilized 2B material is close to the coarser side of the specified gradation band, whereas the distribution curve for the 2B material used in the stabilized asphalt-treated permeable material (ATPM) mix is close to the finer side of the specified band.

Laboratory densities, porosities, and permeabilities are given in Table 1. A source specific gravity of 2.61 was used for all calculations. Naturally, the stabilized aggregate-cement base material had the highest maximum density, lowest porosity, and slowest permeability--of the order of 10^{-7} cm/s. The well-graded standard PA 2A subbase material (control) had the next highest maximum density, a low porosity, and a slow permeability--of the order of 10^{-4} cm/s. The ATPM and HP material had intermediate maximum densities, porosities, and permeabilities, of about 2 and 6 cm/s, respectively. The unstabilized PA 2B material had the lowest maximum density, highest porosity, and fastest permeability--nearly 8 cm/s.

The laboratory permeabilities, except for the aggregate-cement, were determined by standard constant-head test equipment and by falling-head and constant-head testing with a piece of equipment that was fabricated in-house. Because the aggregate-cement was nearly impermeable, its permeability was determined by using core samples set up in a triaxial testing device. Laboratory permeability testing indicated that the specified HP gradation included unnecessary fines. The material finer than approximately the 2.00-mm (U.S. No. 10 standard) sieve size readily migrated within the HP gradation matrix under the imposed hydraulic conditions. This migration of about 5 percent of the material appreciably decreased the measured permeabilities with time as the test progressed.

Field Testing

Field permeability testing was performed by using the field permeability test device (FPTD) developed by Lyle Moulton and Roger Seals at West Virginia University. Schematic diagrams of the water source subsystem and the plate/probe subsystem for this FPTD are shown in Figures 7 and 8. This field testing provided information to statistically compare (a) the laboratory permeabilities to field permeabilities, (b) the variability of permeabilities within a given material section, (c) the variability of permeabilities among the various sections, and (d) the differences in permeabilities measured in two orthogonal directions (90° apart) at the same test location.

Field permeability measurements were recorded at only one location in the PA 2A subbase because of difficulties in obtaining legitimate results at a number of other locations in this material section. A field permeability of 1×10^{-2} cm/s was calculated for one direction and of about 6×10^{-3} cm/s in the orthogonal direction at this one location. Much difficulty was encountered in establishing flow through this layer without the occurrence of piping immediately beneath the plate. It was believed that the field permeabilities of the 2A material (10^{-4} cm/s from laboratory testing) for the most part were near or below the lower testing capability of the FPTD equipment. The recorded measurements at this one location may have been erroneous also or they

may have been factual, indicating a more permeable zone. No field tests were attempted in the impermeable aggregate-cement base layer after the difficulty that was encountered in the moderately slow-permeability 2A material.

Testing the ATPM, the HP material, and the PA 2B coarse aggregate was relatively successful and provided interesting statistical data, which will be discussed in the next section. Tests were made at different locations in each of these sections, and multiple measurements were taken in each of two (K_1 and K_2) orthogonal directions. For the most part, the 45° arrow halfway between these two rows of probes was aligned with the fall line of the grade. The test locations in the ATPM, the HP, and the 2B sections were randomly chosen to provide both longitudinal and transverse coverage of the section material. In-place density measurements were made with a Troxler nuclear gauge at the FPTD test locations. Because of the high void ratio and unconfined instability of the 2B aggregate, field densities were not obtained in this material; however, a density was approximated from laboratory design data. Void ratios (e) and porosities (n) were calculated by using a source specific gravity of 2.61. These field density and porosity data are listed in Table 2.

CONSTRUCTION DETAILS

The entire job, which included the experimental sections, was bid on a competitive basis. The unit prices received from the selected contractor for the different base/subbase materials are as follows (1 in = 2.5 cm; \$1.00/yd² = \$0.83/m²):

Section	Interlayer Only (\$/yd²)	Interlayer and Subbase (\$/yd²)
1, aggregate-cement (6 in)	10.00	13.50
2, ATPM (5 in)	5.40	9.40
3, PA 2B aggregate (8 in)	4.30	6.80
4, HP (8 in)	4.30	6.80
5, PA 2A subbase (8 in)	4.00	6.50

The five sections of different base/subbase materials were constructed in July 1980 without major difficulties or delays even though the contractor was unfamiliar with some of these materials. The 25-cm-thick RCP pavement was placed in August 1980 by conventional fixed-form methods without incident. A 7-m-wide (two lanes) pavement was poured monolithically.

The pavement base drain system was typical throughout all the test sections and was constructed in accordance with recently implemented design and material changes. The longitudinal trench was excavated 33 cm (the depth of the subbase) away from the travel lane and shoulder edge of the pavement in both the northbound and southbound directions on tangent sections. The perforated plastic drain pipe was then placed, and the trench was backfilled with PA 1B crushed aggregate (pea gravel). The plastic drain pipe was 12 cm in diameter, semicircular, and outlets were through the slope or into drop inlets. Outlet spacings ranged from 30 to 182 m and were typically of the order of 91 m. In all cases, the experimental permeable layer was brought into intimate contact with the PA 1B trench backfill mate-

Figure 1. Aggregate-cement test area.

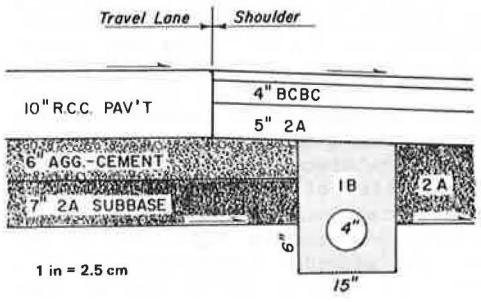

Figure 2. Asphalt-treated permeable material test area.

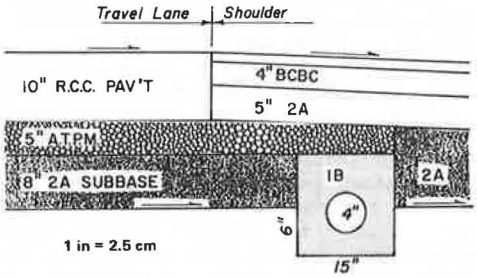

Figure 3. 2B aggregate test area.

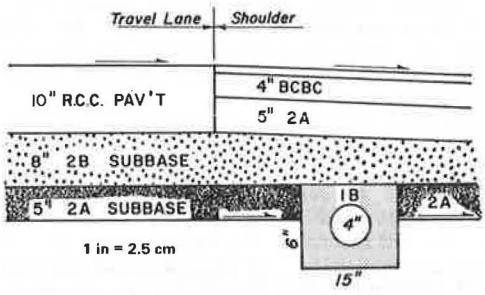

Figure 4. High-permeability test area.

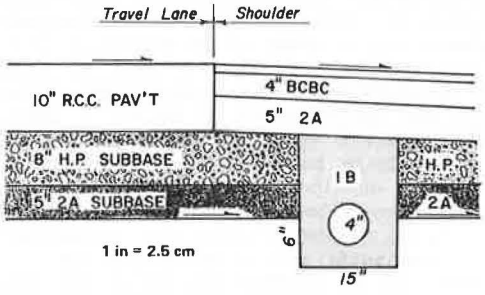

Figure 5. Standard subbase control area.

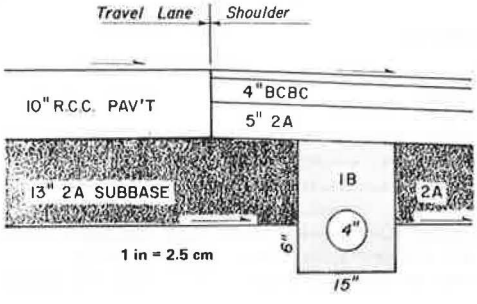

Figure 6. Aggregate gradation bands.

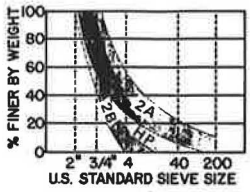

Table 1. Laboratory test data for material types.

Material	$\delta_{d\ max}$ (pcf)	n_{min} (%)	K (cm/s)
Aggregate-cement	138.1	16	1.0×10^{-7} [a]
2A subbase	124.9	23	1.8×10^{-4} [b]
			3.7×10^{-4} [b]
			7.4×10^{-4} [c]
	106.9[d]	34	1.1×10^{-2} [e]
ATPM	112.7	31	2.3×10^{0} [c]
			2.4×10^{0} [e]
HP	110.0	32	6.4×10^{0} [c]
2B subbase	102.9	37	7.6×10^{0} [c]

Note: 1 pcf = 16 kg/m^3.
[a] Triaxial-test permeability.
[b] Standard constant-head permeameter.
[c] Fabricated falling-head test.
[d] Indicates δ_d minimum.
[e] Fabricated constant-head test.

rial to ensure a continuous flow path.

To periodically measure outflow from the base drain system in the various base/subbase sections, 14 accessible outlets were selected for monitoring. Point measurements will be made at various time intervals after rainstorms at these locations. A tipping bucket with a continuously recording counter was installed at the outlet at the downslope end of the ATPM section. This tipping bucket will provide data to determine flow-rate changes with time after rainstorms. A standard weather bureau rain gage was also installed at the site to better predict the infiltration of surface water into the pavement system from these particular rainstorms.

RESULTS

Pavement roughness measurements made on the new reinforced concrete pavement are listed in Table 3 and indicate the paving control afforded by the various bases. The average pavement serviceability indices (PSIs) for the stabilized aggregate-cement and ATPM base sections were 0.2 to 0.3 higher than the unstabilized aggregate base sections. This tends to indicate that these stabilized bases provided a more stable and/or uniform platform on which to pave. The PSI averages for the unstabilized aggregate sections ranged from 3.81 to 3.87, an insignificant difference. This indicates that there was little difference in the contractor's ability to provide a high-quality pavement surface on the PA 2B, the HP, and the PA 2A (control) material sections. Comments regarding the difficulty in maintaining a uniform grade on the PA 2B base appear unfounded when these roughness measurements are compared. PSI measurements made one year after construction indicated the same roughness relationship among the sections as the initial measurements.

A detailed visual inspection of the pavement surface made 15 months after construction revealed that most of the transverse and longitudinal joints were well sealed and in excellent condition. The hot poured sealant was cracked, debonded, or removed on a small percentage of transverse joints. No spalling, faulting, or cracking was encountered.

Statistical methods were applied to the permeability data to calculate the means and deviations of the calculated permeabilities within each test section, to compare the average field permeabilities with the average permeabilities determined in the laboratory, to compare permeabilities in the K_1 and K_2 orthogonal directions at the same location, and to relate the average field permeability with the average material porosity.

The field permeability means and standard deviations for each base material section are given below

Figure 7. Schematic of fresh and salt water subsystem.

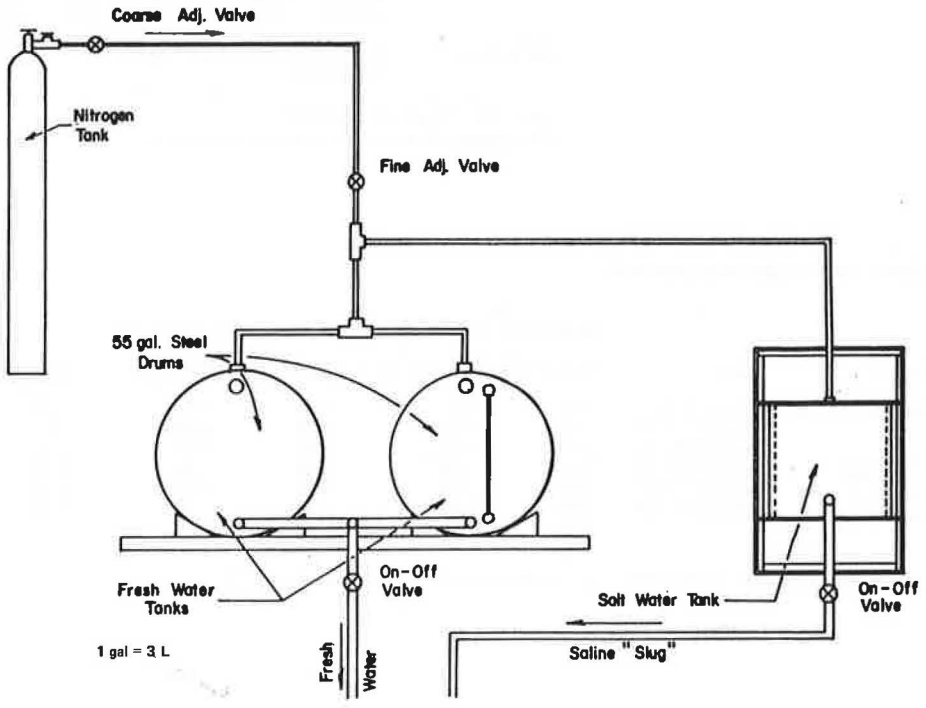

Figure 8. Schematic of plate and probe subsystem.

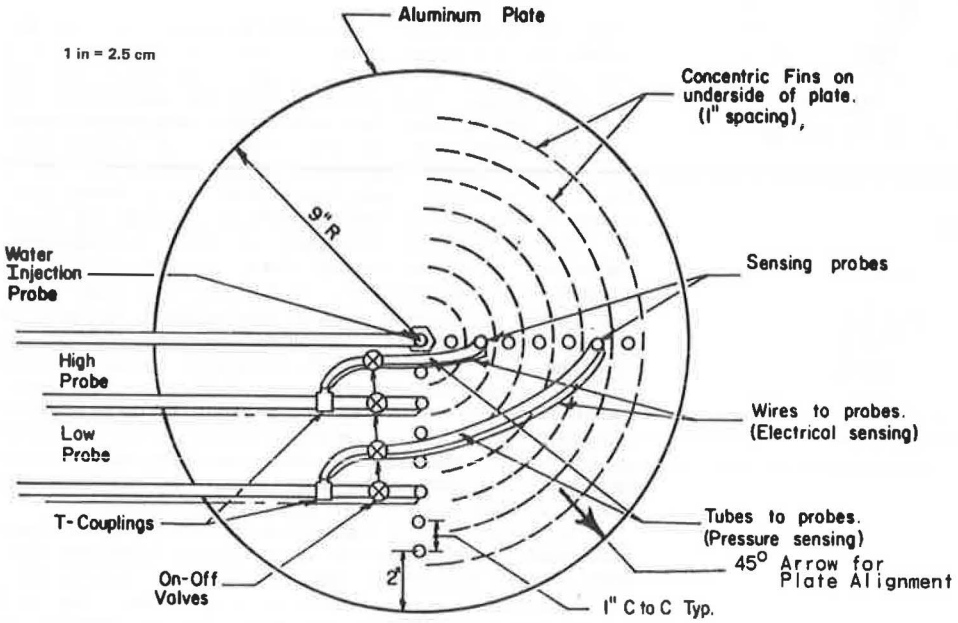

Table 2. Field density and porosity data.

Material	Station	Offset (ft)[a]	δ_w	w(%)	δ_d(pcf)	e	n(%)
Aggregate-cement	Data obtained from mix design testing			–	138.1	0.19	16
2A subbase	731+75	12 R	134.3	6.1	126.7	0.29	22
	738+50	12 L	133.5	6.4	125.5	0.30	23
	739+00	20 R	133.5	7.1	124.6	0.31	23
	754+45	10 R	133.5	7.0	124.8	0.30	23
Avg					125.4		23
ATPM	758+44	26 R	107.8	–	107.8	0.49	33
	768+20	14 R	101.0	–	101.0	0.59	37
	770+85	10 R	106.5	–	106.5	0.51	34
	772+10	19 R	112.1	–	112.1	0.43	30
Avg					106.9		33
HP subbase	829+44	8 R	102.0	7.5	94.5	0.72	42
	829+90	15 R	114.0	7.5	106.5	0.53	35
	830+35	7 R	106.0	6.9	99.1	0.64	39
	831+00	18 R	109.3	7.3	102.0	0.60	38
	833+70	6 R	104.2	6.5	97.7	0.67	40
Avg					100.0		39
2B subbase	Data derived from field concrete design data			–	93.2	0.75	43

Note: 1 ft = 0.3 m; 1 pcf = 16 kg/m^3.

[a]R = right side of pavement; L = left side of pavement.

Table 3. Initial roughness measurements.

		Northbound or Eastbound		Southbound or Westbound		
Material	Station	Travel Lane	Passing Lane	Travel Lane	Passing Lane	Section Avg
Aggregate-cement	125+95-140+09	3.96	4.00	4.02	3.95	3.98
ATPM	758+00-772+50	3.88	4.16	4.14	4.08	4.07
PA 2B	772+50-782+50	3.78	4.00	3.95	3.76	3.87
HP material	822+50-839+75	3.84	3.79	3.83	3.78	3.81
Control A	745+00-758+00	3.93	3.70	3.76	3.84	3.81
Control B	806+00-821+00	3.98	3.62	3.78	3.93	3.83
Avg[a]		3.90	3.88	3.91	3.89	

[a]Average of northbound or eastbound lanes, 3.89; average of southbound or westbound lanes, 3.90.

for both the K_1 and K_2 orthogonal directions:

Material	K_1	K_2
2A	$\bar{X} = 1.4 \times 10^{-2}$	$\bar{X} = 6.3 \times 10^{-3}$
	$S = 0.2 \times 10^{-2}$(?)	$S = 0.1 \times 10^{-3}$(?)
ATPM	$\bar{X} = 1.9$	$\bar{X} = 2.1$
	$S = 1.1$	$S = 1.3$
HP	$\bar{X} = 6.1$	$\bar{X} = 6.3$
	$S = 3.7$	$S = 3.0$
2B	$\bar{X} = 2.7$	$\bar{X} = 8.4$
	$S = 0.7$	$S = 2.3$

The questionable field measurements in the standard PA 2A material (control) indicated the slowest permeability, although the aggregate-cement would obviously have been slower if field measurements had been attainable. The average permeabilities of ATPM, HP, and the PA 2B material were similar and nearly 1000 times more permeable than the dense-graded PA 2A subbase. The means and standard deviations were also very similar for both the K_1 and K_2 orthogonal directions in the ATPM and HP materials. This indicated that, when the average data in these sections are considered, the direction of testing at any test location made little difference. However, there was a significant difference between the means and standard deviations for the K_1 and K_2 directions in the 2B material, thus indicating that directional differences in material permeabilities existed. The HP material exhibited the largest deviation of permeabilities, which indicated the greatest variability between test locations in the same material test section. This variation could be explained by the fact that the 2.00-mm sieve size material was unstable within the total HP matrix. With the segregation of these fines, as noted during laboratory permeability testing and during transport by the producer, varied in-place gradations and hence permeabilities existed in both transverse and longitudinal directions.

The average field and laboratory permeabilities for each material type were compared to determine the relative performance of the FPTD against standard laboratory methods. The correlation coefficient ($R = 0.996$; $m = 0.911$; $i = -0.03$; $n = 4$) for the data shown below indicated a significant correlation at the 99 percent confidence level:

Material	Laboratory Avg (cm/s)	Field Avg (cm/s)
2A	4.3×10^{-4}	1.0×10^{-2}(?)
ATPM	2.4	2.0
HP	6.4	6.2
2B	7.6	6.6

The average permeabilities determined in the field with the FPTD compared very favorably with the average laboratory permeabilities for each of the four material types that were evaluated.

Field permeabilities were compared with the corresponding material porosities calculated from nuclear gauge densities at the test locations. These data showed a significant relationship between permeability and porosity: generally, the greater the porosity, the higher the permeability. The relationship is significant at the 95 percent level of confidence for all points listed above. This good relationship existed in part because all the aggregates came from the same source.

CONCLUSIONS

Base material with significantly higher permeabilities (3 or more orders of magnitude) than the standard PA 2A can be manufactured with adequate quality control at a competitive cost. The contract price for the original standard design of 33 cm of subbase was \$6.50/yd² (\$5.44/m²). The substitution of 20 cm of PA 2B or HP material as an interlayer on top of 12 cm of subbase increased the comparable cost to \$6.80/yd² (\$5.69/m²), about 5 percent more. The substitution of 12 cm of ATPM on top of 20 cm of subbase increased the comparable cost to \$9.40/yd² (\$7.86/m²)--about 45 percent over the cost of 33 cm of subbase. This ATPM cost increase would not be so great in a flexible pavement design where a higher structural coefficient and a decreased required thickness, as compared with the standard subbase, would be used.

Adequate stability to support construction equipment was provided by the more porous, open-graded base materials. All sections of various bases were constructed without major difficulties or delays even though the contractor was unfamiliar with some of these materials. Pavement roughness measurements on the new reinforced concrete pavement indicated that the stabilized aggregate-cement and ATPM sections had PSI values 0.2-0.3 higher than those of the unstabilized or unbounded sections. The PSI values in the unstabilized open-graded materials were equal to or slightly better than the standard PA 2A dense-graded subbase now specified by PennDOT. These same roughness relationships existed after 15 months of service life.

The three open-graded materials had adequately high permeabilities, but the permeability of the PA 2A subbase was unsatisfactorily low. The more porous ATPM, PA 2B, and HP materials exhibited field permeabilities of the order of 10^0 cm/s, whereas the standard PA 2A subbase had measured permeabilities of 10^{-2} to 10^{-4} cm/s. Excellent relationships existed between measured laboratory and field permeabilities for the same materials. Field testing results indicated that permeabilities measured in two orthogonal directions at the same location generally were not significantly different. Permeabilities varied by as much as one order of magnitude within a material section because of gradation segregation resulting from placement practices. The more fines that existed in the material or the more "gap"-graded the material was, the greater was the propensity for this segregation to occur.

Porous material gradations used for drainage interlayers should have minimal material passing the 2.00-mm sieve size. The minus 2.00-mm sieve size material in the HP gradation did not add to the material stability and migrated through the coarser matrix. Even as much as 5 percent of this fine, migrating material could significantly alter the permeability at various locations in the base layer; moreover, it could clog the longitudinal pavement base drain system.

The pavement was performing satisfactorily in all the various base layer sections one year after construction. No distinct differences in pavement performance due to the improved base drainage were evident at that time. Pavement and drainage system performance will continue to be evaluated until a relationship has been determined.

ACKNOWLEDGMENT

The research work described here was done under the sponsorship of the Federal Highway Administration (FHWA) and PennDOT. The contents of this paper reflect my views, and I am solely responsible for the facts and accuracy of the data presented. The contents do not necessarily reflect the official views or policies of FHWA or PennDOT. This paper does not constitute a standard, specification, or regulation.

REFERENCES

1. L.K. Moulton and R.K. Seals. Determination of the In Situ Permeability of Base and Subbase Courses. FHWA, Rept. FHWA-RD-79-88, May 1979.
2. E.B. Drake. Kentucky Highway Project (KY55). Kentucky Department of Transportation, Frankfort, 1979.

Pavement Drainage in Seasonal Frost Area, Ontario

J.B. MACMASTER, G.A. WRONG, AND W.A. PHANG

During the last two decades, full-width granular construction filter courses; improved ditching, trenches, and drains; and axle-load controls have all been implemented on Ontario highways. In spite of this, pavement damage during late winter and spring continues to be a problem for the Ontario Ministry of Transportation and Communications. This paper illustrates how this problem is compounded in seasonal frost areas. During warm winter days, melt-water from deicing salts enters the partly thawed base. Trapped there by frozen subbases and shoulders, it creates differential heaving during subsequent freezing periods. Two experiments carried out to explore the problem of pavement edge cracking are described briefly. These tests include the use of plastic pavement edge skirts and partial-width paved shoulders. The success and practicality of the paved shoulders prompted the Ministry to use them on a continuing basis. The Ministry has been using plastic pipe pavement edge drains since 1978 to improve the drainage of rigid pavements. Details are given on how the drains are placed with trenchless plows; an innovative and very successful installation technique. The Ministry's limited use of open-graded drainage layers is touched on briefly. In the area of preventive maintenance, the discussion centers on preliminary studies on the use of primed and surface-treated shoulders as waterproofing measures. Routing and sealing of cracks has also become a significant feature of the Ministry's program in upgrading the performance of pavements and prolonging the life of overlays.

It is generally acknowledged by highway agencies that, of all the environmental factors that adversely affect the performance of pavements, water is the most significant. Excess moisture in granular base and subbase layers leads to high pore pressures under the dynamic loading of traffic. These high pore pressures tend to overcome the frictional forces between the granular particles and cause a reduction in the bearing capacity of the base. This in turn causes an increase in stress in the wearing course.

Cedergren and Godfrey (1) claim that inadequate drainage of excess moisture in the structural section leads to premature damage of the pavement. Ratios of damage caused by traffic impacts on pavements with free water versus those with little or none and the tests that determined them are as follows: Western Association of State Highway Officials (WASHO) Road Test (2), up to 70 000:1; American Association of State Highway Officials (AASHO) Road Test (3), up to 40:1 (Cedergren analysis of Liddle data); University of Illinois Circular Test Track (4), 100:1 to 200:1 (Cedergren analysis of test data).

In Ontario, as in other seasonal frost areas, weakening of the pavement occurs during the spring when the subgrade begins to thaw. The thaw period can spread over several weeks, particularly in northern Ontario where the frost has penetrated more than 3.0 m (10 ft) below the surface. However, this spring effect may, in the southern parts of Ontario, be repeated several times during the winter, since the base layer is subjected to periodic thaw cycles caused by deicing salts.

In the past 15-20 years, designers have developed various changes in the physical structure of pavements and in the materials used in highway construction. This reflects the attempt to improve the performance of roadways, in part by maintaining a low moisture content in pavement structures.

Subdrains have been installed at various locations within the right-of-way to intercept water that might otherwise enter the base and subbase. Pipes have been located below ditchlines to lower high water tables in the subgrade and cut slopes. Drains have also been placed in the outer edges of the shoulders to help drain the pavement structure when it was impossible to provide side ditches of adequate depth. Such treatments, although effective, were limited in scope and constructed to deal with specific problem locations.

In the early 1960s, the Ontario Ministry of Transportation and Communications (MTC) switched from a core, or earth shoulder, design to full-width granular construction in order to provide lateral drainage of the pavement structure. At the same time, the specifications of the base and subbase materials being used in Ontario were being altered (made more dense) to achieve greater stability to cope with the increasing volume and weight of traffic loads. However, while the densities and bearing capacities of these aggregates were increasing, the permeability values were decreasing, thus reducing the effectiveness of the full-width lateral drainage.

In more recent years, some highway drainage experts have vigorously promoted the use of an open-graded drainage layer within the pavement structure. These layers of materials that exhibit high permeability may be constructed full width and daylighted at the side slopes or designed to outlet into a collector drain installed beneath the shoulder. Cedergren (5) advocates that such a drainage layer have laboratory permeability rates of 6000 m/day (20 000 ft/day) in areas where frost penetrates below the depth of the drainage layer. He cautions, however, that actual field values are likely to be of the order of 2100-3000 m/day (7000-10 000 ft/day).

In this report, experiments are described that demonstrate the pavement structure drainage problem in a seasonal frost area of Ontario and the steps that are being taken to avoid or reduce the damaging effects. These include limited use of very permeable drainage layers but principally relate to provision of partly paved shoulders and pavement edge pipe drains.

SOURCES OF WATER

Although it is known that excess moisture adversely affects the performance of roadways in any climate, pavements in seasonal frost areas are subject to additional stresses at certain times of the year (6).

Figure 1. Snowmelt trapped by plowed snowbanks.

Figure 2. Spring breakup due to poor subsurface drainage.

During the winter, most precipitation remains frozen above ground in the form of ice and snow. Snowbanks created by winter plowing operations tend to restrict the movement of water produced from salting operations or direct sunlight (Figure 1). This melt water remains on the granular shoulders long enough to infiltrate the base and subbase layers and enter through cracks in the pavement. During warm winter days the granular shoulder adjacent to the pavement may thaw slightly, due to the heat-absorbing qualities of the asphalt. The standing water can then penetrate and further saturate the base. While the granular base beneath the pavement thaws, the remainder of the shoulder, insulated by the snowbanks, remains frozen. The result is a trough or bathtub effect in which water is trapped beneath the surface. During the night, this moisture freezes and causes the pavement to heave. Repeated freeze-thaw cycles in late winter and early spring overstress the asphalt and cause longitudinal cracking to develop at the pavement edge. In time, these cracks progress inward toward the wheel-track area and when pavement courses are thin [less than 40 mm (1.5 in)] eventually cause pavement breakup. Frozen drainage ditches can also aggrevate the bathtub effect and result in pavement breakup such as that in Figure 2.

Figure 3. Plastic edge skirts in gravel shoulder.

INVESTIGATION OF TREATMENTS AND PARTLY PAVED SHOULDERS

In southwestern Ontario, a study of thin asphalt surfacing failures resulting from edge cracking indicated that moisture was entering the base via the shoulder and causing excessive heaving of the asphalt (7). Experiments were conducted to see whether directing the water away from the pavement edge would improve the performance.

Pavement Edge Skirts

In this test, 0.2-mm (8-mil) polyethylene sheeting was draped into a shallow trench excavated in the shoulder (8). One edge of the sheeting was tacked to the old surface with asphalt cement and then covered with a strip of natural rubber membrane 0.3 m (1 ft) wide to provide protection against the hot overlay (Figure 3). The trench was backfilled and the roadway resurfaced. Monitoring consisted of crack surveys, deflection measurements, and measurements for frost heaving.

Partly Paved Shoulders

This experiment was carried out on a newly constructed county road. Through the test section, the 40-mm lift of asphalt was extended by 0.9 m (3 ft) on either side of the two-lane road. Monitoring was similar to that carried out in the skirted sections. The most significant results concerned the heaving pattern of the pavement within and adjacent to the test sections in both experiments. As shown in Figure 4, the skirts and partly paved shoulders produced similar results. Not only was the magnitude of heaving reduced in each case, but the differential heaving between the central portion of the roadways and the edges of the pavement was significantly reduced.

These results confirmed that (a) much of the excess moisture that enters the pavement structure

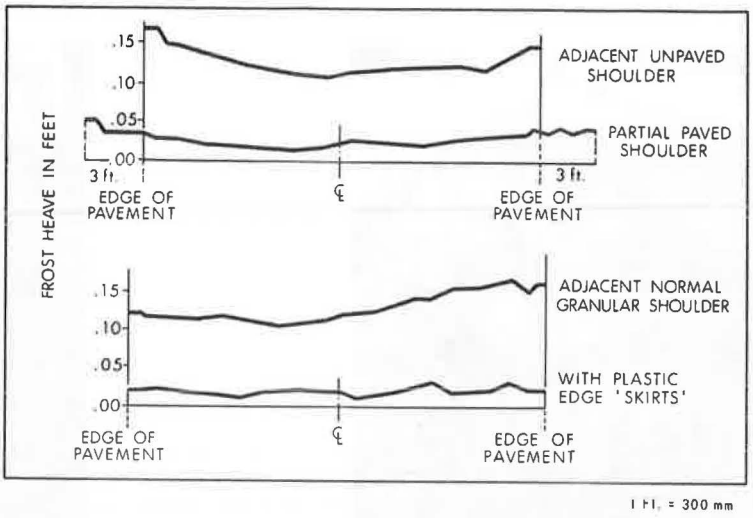

Figure 4. Cross-section heave measurements at partly paved shoulder and skirt sections.

does so from the surface and (b) changing the flow pattern of this surface water reduces the detrimental effects of frost on the pavement, especially at the point where wheel loads are greatest.

Paved Shoulders

While the preceding experiments produced similar results, economics dictated that, for province-wide applications, placing a single lift of asphalt concrete 0.6 m (2 ft) wide on the existing gravel shoulder adjacent to the driving lane was a more feasible treatment. The 0.6 m served nearly as well as 0.9 m in keeping surface water away from the pavement edge. MTC has constructed partly paved shoulders for the past four years in accordance with criteria listed below; fully paved sholders are used in urban freeway sections where traffic volumes exceed 20 000 annual average daily traffic (AADT):

1. Two-lane highways where AADT = 4000 within next five years,
2. All four-lane undivided highways,
3. Four-lane divided highways where AADT = 20 000 within next five years,
4. All of TCH-401,
5. Route continuity, and
6. Special locations determined by highway accident rate and high maintenance demand.

Partly paved shoulders are generally placed when resurfacing is scheduled and are constructed integrally with the traveled lanes. In 1980, problems occurred on some resurfacing projects in Eastern Ontario when the edges of partly paved shoulders, paved to the same crossfall as the driving lane (2 percent), heaved to such an extent that water was trapped on the driving lane. This prompted the construction of experimental sections on TCH-17-N near Petawawa. With the use of a new, adjustable screed extension, 0.6-m partly paved shoulders were placed at 2 and 6 percent crossfall. No construction problems were encountered in placing the shoulders at 6 percent crossfall, and measurements taken through the following winter and spring revealed that, although some heaving did occur, the shoulders always maintained a positive crossfall.

Assured that there would be an adequate supply of screeds available to accommodate paving contractors, MTC issued a directive in June 1980 stating that partly paved shoulders would be laid at 6 percent crossfall in the future.

PAVEMENT STRUCTURE DRAINAGE SYSTEMS

Pavement Edge Drains

Poor pavement performance is not restricted to conventional flexible pavement structures. Rigid structural sections, such as portland cement concrete and composite designs, develop distresses that can be attributed to excess moisture within the base and subbase layers. Common distresses include faulting at joints and cracks, settlement and corner cracking of slabs, and deterioration of the underside of the concrete.

In the early 1970s, the above problems were becoming prominent on concrete pavement in Ontario. Most of the concrete pavements under the jurisdiction of MTC are found on expressways and multilane facilities such as TCH-401. Surveys carried out in southwestern Ontario revealed multiple transverse cracking and serious deterioration of the underside of the slab. Breakdown of the concrete was quite prominent at joints. Free water was discovered beneath the pavement in many areas, which lent support to the opinion that the permeability rates of bases and shoulders are not high enough to permit proper lateral drainage of the structural section. It was evident that in order to prevent complete failure of the pavement and prolong the service life of rehabilitative treatments, some form of continuous drainage system was required.

A survey carried out by AASHTO in 1975 (9) revealed that a small number of states were installing edge drains to provide drainage for transportation facilities. Polyethylene pipe appeared to be the most common type of drain used. Some states employed equipment such as chain or wheeled trenchers with automatic backfilling apparatus capable of placing an envelope of free-draining filter material around the pipe.

In 1976, MTC investigated the possibility of installing subdrains along the edges of concrete pavements. The pipe chosen was 100-mm (4-in) perforated polyethylene tubing. In order to keep installation costs down, it was decided to place the tubing in the shoulder by using a trenchless plow (Figure 5). Both tubing and plow are quite familiar in the area of farm drainage.

An 0.8-km (0.5-mile) test section was constructed on TCH-401 near Chatham, Ontario (10). Polyethylene tubing 100 mm in diameter wrapped in a knotted polyester filter sock was plowed into the shoulder at

both edges of the 7.2-m (24-ft) concrete pavement. The drains were offset about 0.3 m (12 in) from the edge of the slab and located at subgrade level so that the pipe had about 0.5 m (20 in) of cover. No attempt was made to place any special backfill around the pipe, and outlets were provided at 75-m (250-ft) intervals. Results were evident almost immediately. Discharge was noted by maintenance staff on a regular basis during the summer and fall (Figure 6).

Figure 5. Installing plastic pipe subdrains by using trenchless plow.

Figure 6. Discharge from pavement edge subdrain.

Figure 7. Layout of pavement edge subdrain system.

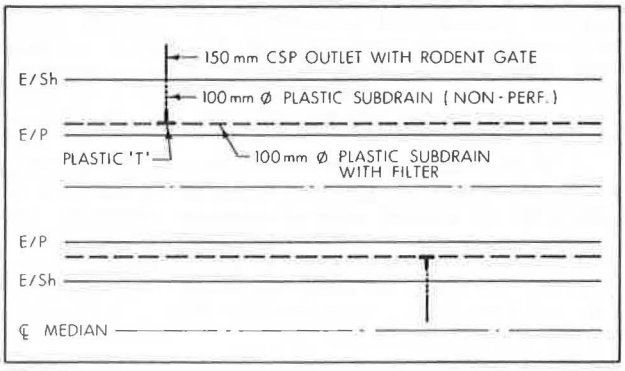

Encouraged by the performance of the drains and the potential of the plowing technique, the Ministry included subdrains on a 23-km (14-mile) resurfacing contract the next year. By using a tracked plow and four backhoes, the contractor installed 96 900 m (323 000 ft) of perforated tubing and 2370 m (7900 ft) of nonperforated outlet tubing in five working days. Changes were made to the plowing technique to increase production. Rather than plowing in individual lengths of tubing [75 m (250 ft)], the contractor joined the rolls to form one continuous run. This allowed the operator to plow without stopping until an interchange or bullnose was encountered. The main line was then tapped at the desired interval by a backhoe and outlet tubing connected with special T-couplers (Figure 7).

The installation of plastic subdrains by plowing has now become a standard feature of concrete pavement rehabilitation in rural areas. Several contracts have been awarded for pavement drainage in advance of resurfacing projects. The cost of installed pipe, including outlets, averages $1.90/m ($0.57/ft). Since the initial contract referred to above, a total of 981 000 m (3 270 000 ft) of perforated plastic tubing with filter wrap has been placed by MTC. This accomplishment is summarized by year below (1 km = 0.6 mile):

Year	No. of Contracts	Plowed Subdrains (km)	Outlet Pipe (km)
1978	4	270	5.3
1979	6	675	9.8
1980	4	187	3.0
1981	3	274	6.3

On recent projects, tracked plows have been replaced by rubber-tired units (Figure 8). This move has increased average daily production from 16 to 23 km (10-14 miles). In addition to providing operator comfort, the new method is advantageous because the pavement surface is no longer marred by the steel tracks. Tubing is now supplied in 1200-m (4000-ft) rolls, thus reducing the handling required.

To date, priority has been given to draining beneath concrete pavements. Investigations have shown, however, that excess moisture is also present within composite pavement structures (asphalt over concrete base over cement-treated granular subbase). Moisture infiltration in composite pavements is serious because water contaminated with salt attacks the cement-treated subbase. A total of 200 130 m (667 100 ft) of subdrain pipe was plowed in composite pavements in 1981.

The use of plastic subdrains for pavement drainage has proved to be quite successful in Ontario due to the low cost of materials and the ease of construction. Such a system could be adapted to flexible pavements. Full-depth and deep-strength asphalt pavements are currently under review to determine whether edge drains are required.

Our pavement edge drains, prior to 1981, were all retrofits to existing facilities. On two contracts recently completed, edge drains were incorporated into the pavement structure at the design stage (Figure 9). This represented the Ministry's first effort at providing a built-in drainage system.

The long-term performance of underdrains is often questionable. Examination of this type of pipe after four years in service has shown no deterioration of the pipe or clogging of the filter sock. Over this same period, no change in discharge rates has been observed, either in the experimental sections or in the runs subsequently placed.

Figure 8. Trenchless plow mounted on rubber-tired tractor.

Figure 9. Plastic edge drains located in new composite pavement.

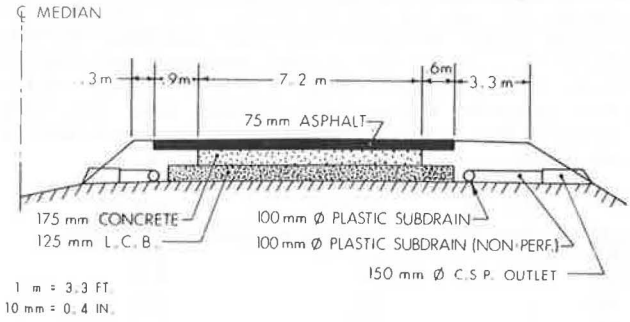

Open-Graded Drainage Layers

As noted earlier in this paper, much attention has been given to the construction of highly permeable drainage layers within the pavement structure. Johnson (11) suggests that in frost areas this open-graded layer should be located in the upper portion of the structural section, preferably beneath the wearing course.

Figure 10 illustrates gradation curves for typical aggregates necessary to achieve the permeability rates advocated by Cedergren (5). Superimposed on this chart are Ontario's specifications for the granular base course ("Gran. 'A'"). It is evident that with this material located below the asphalt wearing course, water will remain in the pavement structure for some time.

In 1975, the Ministry constructed a series of test sections that incorporate an open-graded drainage layer. The site of the experiment was a new section of two-lane highway near Stoney Creek in southern Ontario. The designed pavement structure consisted of 125 mm (5 in) of asphalt concrete over 525 mm (21 in) of granular A base. The drainage medium was the course aggregate used in HL 8 asphalt concrete (Figure 10). In the first test area, the upper 75 mm (3 in) of base was replaced with a similar depth of the above stone. The second test area was identical to the first except for the addition of 3 percent asphalt cement as a binder. The third trial section contained 150 mm (6 in) of untreated stone. Apart from movement of untreated stone under construction traffic, no problems were encountered during construction.

Monitoring data has indicated some settlement problems in test section 3. Investigations will be under way shortly to determine the reason for this problem. Cracking is more extensive over the 150-mm layer of stone than in the other two test areas. The small amounts of cracking in the first and second test sections are quite similar.

Data will have to be fully analyzed before definite conclusions can be made as to the effectiveness of the drainage layers.

Figure 10. Permeability of granular A base: Ontario specification.

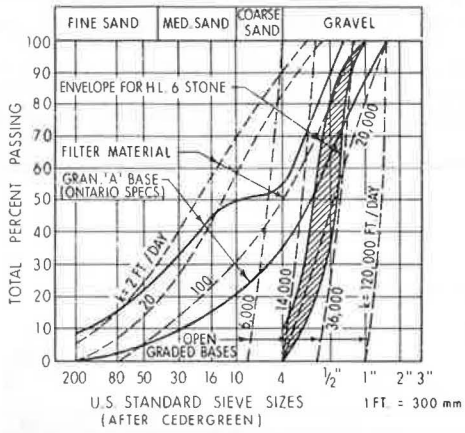

Figure 11. Primed gravel shoulder three years after application.

WATERPROOFING

Shoulder Treatments

Although a good deal of effort is being expended in developing means to remove excess moisture from pavement structures, attention also needs to be directed toward the prevention of surface water infiltration. The sealing of permeable surfaces would appear to be a logical step in this direction since it has been shown that a good deal of water enters the base through the shoulder at the edge of the pavement.

In 1977, the Ministry constructed test sections at several sites in southern Ontario as part of an experiment to control edge-of-pavement dropoff. One of the treatments applied was RC-30 prime over a 0.9-m width of shoulder next to the pavement. After three years, much of this treatment was still in place (Figure 11). Its potential for waterproofing purposes is now being studied.

During the winter of 1978-1979, heaving of partly paved shoulders on an expressway occurred near

Ottawa, indicating that moisture was entering the base. In an effort to seal the remaining 3.0 m of granular shoulder, the maintenance staff applied a surface treatment consisting of a high-float emulsion and 16-mm (0.625-in) crushed gravel. This treatment has been in place for two years and is still in very good condition. No further heaving of the partly paved shoulders has taken place.

Where infiltration of moisture on gravel shoulders is creating deterioration of the pavement, waterproofing of the shoulder by either priming or surface treatment is considered as a preventive-maintenance measure.

Routing and Sealing Cracks

Dense-graded asphaltic concrete pavements are relatively impermeable for a period of time following construction. In time, cracks develop in various forms in overlays and in pavements placed on new grade. These cracks represent a very significant source of entry for surface water. Studies have shown that up to 70 percent of surface runoff can enter a crack no wider than 0.8 mm (0.031 in) (1).

Treatment in past years usually consisted of spray patching and sand sealing when the severity of the cracks caused a decrease in riding comfort or threatened the integrity of the pavement. Such treatment was successful, although usually for only a short time. Fillers became displaced, and in many cases riding comfort was affected by a buildup of sand in the vicinity of the crack.

In the last four or five years, new sealing compounds have been developed that are designed to penetrate and adhere to the sides of the crack. They compress or stretch as the crack closes or opens with changes in temperature. The product is delivered in cake form and is then melted down in large kettles.

In order to provide a reservoir to ensure that there will be sufficient sealant to fill the crack properly, it is routed and cleaned with compressed air prior to filling. Experience has shown that, usually, a 16x16-mm opening is adequate. For wider cracks that develop over bases such as cement-treated granular, an opening of 19x19 mm (0.375x 0.375 in) may be required. The routed crack is overfilled rather than underfilled.

The success rate of the Ministry's sealing program has been encouraging. Contracts have been awarded specifically to explore the suitability of available sealants. Work is scheduled when the cracks have opened sufficiently to permit routing. The importance of preventing the infiltration of surface water in the pavement structure justifies the need to return to sections of highway more than once, as cracks develop. A large number of maintenance patrols are now equipped to carry out crack sealing. The Ministry is currently considering tendering contracts that would contain a lump sum of money designated for crack sealing a year or two after construction.

The Ministry is also engaged in evaluating new crack-sealing products as they become available. Test sections have been established and manufacturers invited to supply and supervise placing of their sealants. The trials are being monitored to compare the effectiveness of these treatments under similar field conditions.

CONCLUSIONS

Since the performance and ultimately the life of a pavement can be appreciably curtailed when excess moisture exists within the base and subbase, it is imperative that every effort be made to keep surface water out of the pavement structure. Although base courses have been upgraded to provide increased stability, the drainage characteristics have often been adversely affected.

Experiments carried out by MTC have shown that in frost areas, infiltration of surface water has had a detrimental effect on pavement performance. Where moisture has been diverted away from the pavement, heaving and distortion of the asphalt have been dramatically reduced. Plastic edge skirts, although showing promise in achieving this result, have given way to the more practical and cost-effective partly paved shoulder.

The use of plastic edge drains has become a major feature of the Ministry's pavement drainage scheme. Their low cost and ease of installation by plowing have made them an attractive system for all types of pavement structures.

Open-graded drainage layers have had a limited application to date in Ontario; nevertheless, MTC will continue to evaluate this method of drainage and modify current designs to achieve an efficient system.

From the point of view of preventive maintenance, crack sealing is being actively implemented in many districts. Priming and surface treating of gravel shoulders have been recent innovations, but they show excellent potential as interim measures to redirect surface water.

The cost of constructing and maintaining a highway system continues to escalate as supplies of good-quality aggregates diminish and petroleum products increase in cost. Providing adequate drainage of the pavement structure to prolong pavement life is a major step toward protecting the investment made in a highway network. MTC is actively addressing this problem and will continue its efforts to improve and develop drainage designs and systems to achieve this goal.

REFERENCES

1. H.R. Cedergren and K.A. Godfrey, Jr. Water: Key Cause of Pavement Failure. Civil Engineering, Sept. 1974.
2. The WASHO Road Test, Part 2. HRB, Special Rept. 22, 1955.
3. W.J. Liddle. Proc., 1st International Conference on the Structural Design of Asphalt Pavements. Univ. of Michigan, Ann Arbor, 1962.
4. E.J. Barenberg and M.R. Thompson. Highway Engineering Series 36, Jan. 1970.
5. H.R. Cedergren, K.J. O'Brien, and J.A. Arman. Guidelines for the Design of Sub-Surface Drainage Systems for Highway Structural Sections. FHWA, Rept. RD-72-30, June 1972.
6. G.A. Wrong, W.A. Phang, and G.M. Stott. Roadway Drainage in Seasonal Frost Areas. Presented at Annual Conference of Roads and Transportation Association of Canada, Calgary, Alberta, Sept. 23-26, 1975.
7. W.A. Phang and G. Chong. Thin Asphalt Pavements--A Performance Study. Ontario Ministry of Transportation and Communications, Downsview, Ontario, Res. Rept. IR 53, Feb. 1974.
8. J.B. MacMaster. The Use of Plastic Pavement Skirts to Eliminate Pavement Edge Cracking. Engineering Materials Office, Ontario Ministry of Transportation and Communications, Downsview, Ontario, Rept. EM-25, March 1979.
9. Plastic Pipe for Sub-Surface Drainage of Transportation Facilities. NCHRP, Rept. 225, 1980.
10. J.B. MacMaster. A Study on Improving Pavement Drainage Using Plastic Pipe Sub-Drains. Engineering Materials Office, Ontario Ministry of Transportation and Communications, Downsview,

Ontario, Rept. EM-10, Feb. 1978.
11. T.C. Johnson. Is Graded Aggregate Base the Solution in Frost Areas? Proc., Conference on Utilization of Graded Aggregate Base Materials in Flexible Pavements, Oak Brook, IL, March 1974.

Simulating Pavement Performance Under Various Moisture Conditions

MICHAEL J. MARKOW

A computer program to simulate highway pavement performance, maintenance, and rehabilitation has recently been completed for the Federal Highway Administration. As part of this effort, closed-form pavement performance equations have been incorporated to predict the onset and propagation of various damage mechanisms as a function of layer thicknesses and material properties, traffic loadings, cumulative damage already sustained, moisture, and temperature. Both flexible and rigid pavements are considered. The simulation is carried out on a seasonal basis (up to 12 seasons per year allowed) to permit users to specify variations in climatic conditions and pavement material properties. In addition, moisture-induced decreases in layer and subgrade strengths are rendered sensitive to the amount of unsealed cracking in the pavement surface, the seasonal rainfall, and the quality of subsurface drainage. In this way the preservation of road investment, as represented by rates of future damage accumulation, is explicitly tied to both pavement drainage characteristics and the quality of subsequent surface maintenance. This paper describes the technical assumptions and relationships employed in this approach and gives examples of its application to a selected pavement design, maintenance policy, and climatic region. The case study indicates that subsurface drainage above can have a significant effect on pavement life, influencing the date of required resurfacing by up to four years.

The structural design, construction, and performance of pavements have been the subject of much theoretical and empirical research. Most efforts in this area have concentrated on the relationship of component layer thicknesses and material properties to the formation and propagation of particular types of distress. Comparatively little attention, however, has been devoted to the changes in pavement condition over time as damage begins to accumulate and the interaction between this damage and the pavement environment to influence subsequent pavement performance. The specific mechanism of interest here is the infiltration of water into cracks and joints, with resulting potential weakening of the pavement structure. This mechanism is important because a good deal of structural maintenance and rehabilitation is devoted to preserving the integrity of the pavement surface. The benefits of such work are often justified in part by the reduction in water infiltration, but typically no quantitative evidence of impacts on future pavement damage is provided.

The lack of current information on the effects of water infiltration and drainage has been cited by Cedergren (1). By using data from several road tests and test tracks, he calculated relative damage factors, which ranged from 5 or 10 to 1 to 70 000 to 1 for wet versus dry conditions, respectively. Although the trend indicating shortened pavement life with increasing traffic loads under wet conditions is clear, the wide range of these estimates precludes their applications to predicting pavement performance.

Recently modifications have been completed of the Federal Highway Administration's EAROMAR system--a simulation model of freeway performance that enables one to conduct economic analyses of different strategies for roadway and pavement reconstruction and pavement reconstruction, rehabilitation, and maintenance (2). As part of the simulation of pavement performance, we have included models of water infiltration to the pavement substructure, its effect on material properties, and resulting changes in damage accumulation. The approach followed within EAROMAR bases the amount of water entering the pavement structure on the seasonal rainfall and the extent of cracking in the pavement surface. Reduction in pavement strength is dependent on the length of time the sublayers remain saturated, which is a function of the amount of water that has entered the pavement and the drainage characteristics of the sublayers input by the user. The model considers only water entering the pavement structure through discontinuities in the surface (typically the most significant source); groundwater sources and side infiltration are not included. The technical relationships employed are based on work by Moulton (3) supplemented by data presented by Cedergren (1) and by assumptions on pavement material behavior.

GENERAL MODEL CONSIDERATIONS

In pavements subjected to rainfall, one may distinguish three periods associated with wet weather in addition to the period corresponding to dry conditions:

1. The time during which rain is falling, in which the pavement sublayers may or may not be building up to saturation;
2. If rainfall is sufficiently heavy or the sublayers are of sufficiently low permeability, the time during which the sublayers are saturated or sufficiently wet to affect material properties and structural behavior; and
3. The time during which any residual water not sufficient to affect pavement behavior is drained off.

Data for several cities throughout the United States were reviewed in their months of maximum rainfall. Seldom do the total days of precipitation greater than 0.1 in (2.5 mm) exceed 10, and the number of days in which the precipitation exceeds 0.5 in (12.7 mm) is typically 7 or fewer. However, the period of saturation following a rain can last from 5 to 20 days, except in those pavements that have exceptionally good drainage qualities (1). Therefore, in our model we considered only the second period above--the period (after it stops raining) during which the pavement is significantly

wet or saturated--as the time relevant to estimating changes in rate of pavement damage and neglected the time during which the rain is actually falling (period 1 above). (This assumption was made to simplify the model derivation; there is no reason why the time during rainfall could not also be included if desired.)

Drainage characteristics of pavement sublayers are specified to EAROMAR by qualitative descriptors--good, fair, or poor. For use in the drainage model these descriptions must be reduced to quantitative measures of subsurface permeability. Cedergren (1) presented coefficients of permeability for standard bases and subbases of about 0.02-20 ft/day (0.6-610 cm/day) and for open-graded bases of about 3000-250 000 ft/day (900-75 000 m/day). Based on these data we defined the following correspondence between user descriptions of drainage quality and coefficient of permeability used in model calculations:

Poor: 0.1 ft/day (0.03 m/day),
Fair: 100 ft/day (30.5 m/day), and
Good: 10 000 ft/day (3050 m/day).

Thus, typical bases and subbases used in flexible and rigid pavements today lie in the poor to fair range under this designation.

Quantifying the deleterious effects of water on pavement life requires estimates of (a) the reduction in sublayer material properties during the time the pavement is significantly wet and (b) the duration of this period of weakened strength (in terms of the three wet periods described earlier and the length of time between the starts of the second and third periods, respectively). Unfortunately, the answers to these key questions are not well supported by field documentation.

Von Quintus and others (4) presented data on seasonal changes in plate-bearing capacity for a pavement that had a granular base, frost-susceptible subgrade, and high water table. Based on the September bearing strength normalized to a value of 100, seasonal variations at this site ranged from about 20 in the spring-thaw months to more than 140 in the frozen winter months. Values of relative damage factors between wet and dry periods were discussed earlier; Cedergren (1) calculated values of about 10 to 40 to 1 for the AASHO Road Test. However, these data are not tied to detailed material properties. We have therefore assumed that, during the time of substantial pavement wetness, individual subsurface layer moduli are reduced by 50 percent.

Determining the time during which the pavement is sufficiently wet to affect performance is more difficult. Equations are available that relate degree of drainage (i.e., percentage of water removed from a saturated layer) to time, but again these data are not tied to changes in layer material properties or pavement performance. As a conservative estimate we have calculated drainage times on the basis of an assumed degree of drainage of 0.8. The implication of this and the preceding assumption is that in the time required to drain 80 percent of the water from a saturated layer, the sublayer moduli will be considered to be reduced in value by 50 percent in the EAROMAR simulation.

Based upon these general formulations, the following model relationships were derived.

ESTIMATES OF DURATION OF PAVEMENT WETNESS

The duration of pavement wetness is determined by the interaction of water inflow and outflow characteristics of the pavement structure. As explained in the preceding section, outflow characteristics dominate the particular model within EAROMAR, and it is these relationships that will be explained first. Following the description of outflow equations, we will consider the influence of inflow parameters on the model.

The time required to drain a saturated subsurface layer is captured within the relationships shown in Figure 1 (3). The normalized time factor (t/m) is dependent on the degree of drainage achieved (U), the width of road to be drained (L), the depth of the drainage layer (H_d), and the transverse slope of the drainage layer (S:1). From our earlier discussion, we have assigned a value of 0.8 to U, taken to be the point at which wetness no longer affects pavement structural behavior. Pavement cross slopes typically vary from 0.125 to 0.25 in/ft (1-2 cm/m); we have therefore taken the slope factor (S) to be a constant equal to 0.015. Also, we have taken L conservatively to be equal to the sum of the widths of all lanes plus shoulders in the roadway. Finally, we have assumed H_d typically to be about 1 ft (0.3 m). Based on these assumptions, we fit the following function to data points generated from Figure 1:

$$t/m = 2.5 \exp(-2S') \quad (1)$$

$$S' = 0.015L/H_d \quad (2)$$

$$L = (N_{lanes} \times W_{lane}) + \Sigma W_{shldr} \quad (3)$$

where

t/m = normalized time of drainage;
H_d = thickness of the drainage layer, assumed to be 1 ft;
N_{lanes}, W_{lane} = number and width in feet, respectively, of lanes in this roadway; and
W_{shldr} = widths in feet on the left and right shoulders in the roadway.

The denominator of the normalized time is a function of the yield capacity of the drainage layer:

$$m = nL^2/k_d H_d \quad (4)$$

where

m = normalizing factor;
n = yield capacity (effective porosity) of drainage layer;
L = width of roadway drained, defined by Equation 3; and
k_d = coefficient of permeability of pavement drainage layer.

Values of n can be estimated from Figure 2 (3) by using the coefficients of permeability assigned earlier to users' qualitative descriptions of drainage, as shown below (1 ft/day = 0.3 m/day):

Drainage Quality Input	Coefficient of Permeability k_d (ft/day)	Yield Capacity n
Good	10^4	0.23
Fair	10^2	0.08
Poor	10^{-1}	0.055

With these values one can solve Equation 4 for m and determine t/m from Equation 1. The time of drainage corresponding to the period in which we have assumed that pavement structural behavior is affected is then given by the following:

$$t_{drain} = m(t/m) \quad (5)$$

Figure 1. Time-dependent drainage of saturated layer.

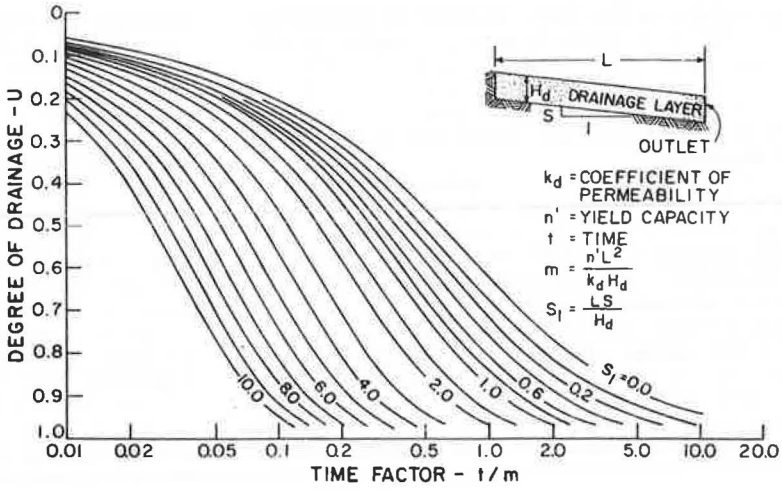

Figure 2. Chart for determining yield capacity (effective porosity).

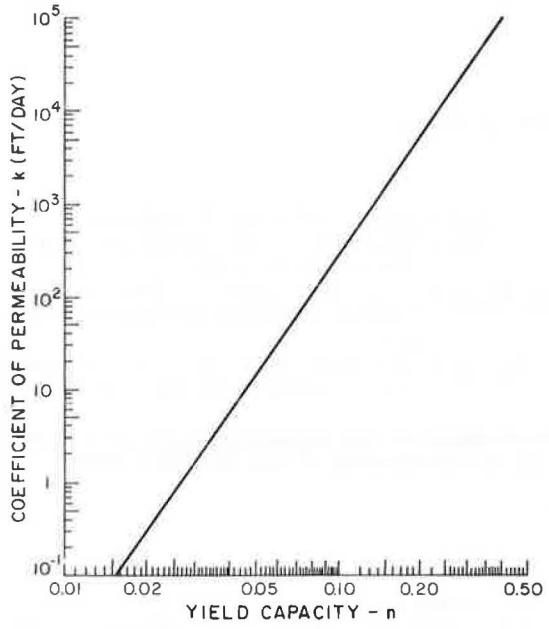

Table 1. Rainfall data for selected cities in peak month of 1978.

City	Total Precipitation (in)	Days of Precipitation	Avg Daily Precipitation (in)
Boston	8.12	15	0.54
San Francisco	6.20	16	0.39
Seattle	6.05	16	0.38
Los Angeles	7.70	10	0.77
Miami	2.57	11	0.23
Chicago	6.38	12	0.53
New Orleans	12.53	17	0.74

where t_{drain} is the time to achieve a degree of drainage of 0.8 in days and m is the normalizing factor computed in Equation 4.

COMBINING INFLOW AND OUTFLOW CONSIDERATIONS

Equation 5 gives the drainage time of a saturated pavement layer once the rainfall has stopped. However, the quantity of water to be drained depends not only on the seasonal rainfall but also on the condition of the pavement surface (the number of open cracks and joints). We have treated both these contributing factors to inflow as multipliers of the time computed in Equation 5. Thus, if either the seasonal rainfall (for a fixed amount of cracking) or the amount of cracking or open joints (for a fixed seasonal rainfall) increases, the time during which pavement structural response is affected will also increase. If either the seasonal rainfall or the open cracks and joints in the pavement are negligible, the time the pavement is affected will also be negligible.

Consider first the effects of seasonal rainfall. To convert total precipitation to an equivalent time or duration comparable with the duration predicted in Equation 5, we require an assumed rainfall intensity. Data in Table 1 and reported by Cedergren (1) and Moulton (3) suggest that a daily intensity of 0.5 in/day (12.7 mm/day) is reasonable as a composite national figure.

Findings reported by Cedergren (1) showed that substantial quantities of water can enter even very narrow cracks in a pavement under field test conditions. [Cracks 0.125 in (3 mm) wide admit more than 95 percent of water falling at an intensity of 2 in/h (50 mm/h), even with steep pavement transverse slopes. Cracks as narrow as 0.035 in (0.89 mm) can absorb 70 percent or more of runoff at the same intensity.] In practice these rates may be reduced somewhat, due to debris at the bottom of the crack or to buildup of water in the crack. Nevertheless, infiltration rates become quite high at low levels of cracking or open joints in the pavement surface.

To model this relationship we have assumed the fraction of water inflow to be a negative exponential function of cracking and open joints subject to assumed boundary conditions. Specifically, if there are no open cracks or joints in the pavement surface, water infiltration is reduced to zero. At cracking (or open joints) covering 50 percent of the pavement surface (a highly cracked pavement), infiltration is assumed to equal 99 percent of all water falling on the pavement area.

By combining the above assumptions and incorporating a definition of the total area of discontinuities in the pavement surface, we obtain the following relationships:

$$t_{wet} = (r_{season}/i_{avg})\,[1 - \exp(-9C)]\,t_{drain} \quad (6)$$

$$C = (1/5280)\left\{[(LCRACKS + ACRACKS)/W_{lane}] + [(SHOULDER \times W_{wet})/2W_{lane}N_{lane}] + (JOINTS \times W_{wet})\right\} \quad (7)$$

where

t_{wet} = duration of pavement wetness in days during which structural response is assumed to be affected;
r_{season} = seasonal rainfall in inches input by the user;
i_{avg} = daily rainfall intensity, assumed to equal 0.5 in (12.7 mm);
C = fraction of pavement area having cracks or open (unsealed) joints;
t_{drain} = time in days to drain the saturated pavement sublayers;
LCRACKS, ACRACKS, SHOULDER, JOINTS = quantities of damage components per lane mile computed by pavement simulation models within EAROMAR;
W_{lane}, N_{lane} = width of lane in feet and number of lanes in roadway, respectively, as input by user; and
W_{wet} = width of subsurface zone wetted by open joint, assumed to be 6 ft (1.8 m).

REDUCTIONS IN PAVEMENT STRENGTH

Pavement characteristics simulated within EAROMAR are affected by water infiltration in two ways. First, the strengths of granular bases and subgrades are reduced by 50 percent, as described in the general model formulation. Second, the American Association of State Highway and Transportation Officials (AASHTO) regional factor is adjusted to reflect saturated conditions above and beyond those assumed by the user in initial program input. Resulting model relationships are as follows:

$$F_{red} = (t_{season} - 0.5t_{wet})/t_{season} \quad (8)$$

$$R' = [5t_{wet} + R(t_{season} - t_{wet})]/t_{season} \quad (9)$$

where

F_{red} = reduction factor applied to moduli of granular pavement layers and to California bearing ratio (CBR) and moduli of subgrade,
t_{season} = length of season in days determined from season information input by user,
t_{wet} = duration of pavement wetness in days computed from Equation 6,
R' = AASHTO regional factor corrected for additional wetness due to cracked pavement surface, and
R = regional factor input by user.

Note that Equations 8 and 9 apply a time-average correction (under wet versus dry conditions) to the pavement material properties and regional factor. Multiplication by 0.5 in Equation 8 reflects the assumed loss in material strengths under wet conditions; the coefficient 5 in Equation 9 reflects the value of the regional factor associated with saturated conditions.

The effects of water infiltration on pavement performance are therefore modeled within EAROMAR through the material-related and environmental adjustments indicated above. This makes it possible to consider interactions between load-related and environmental influences on pavement damage and to see what effects unsealed cracks and joints have on the rate of future pavement damage. The latter relationship in turn allows one also to investigate the benefits achieved through the routine maintenance actions of sealing joints and cracks. Predictions of these models applied to a case study are described below.

CASE STUDY

To investigate the trends predicted by Equations 1 through 9, we applied the EAROMAR system to simulate pavement performance and costs on three roadways, each 10 miles (17 km) long, all having identical pavement, traffic, and maintenance policies but differing in drainage characteristics. The deterioration of the pavements was estimated by using damage models described by Markow and Brademeyer (2). Maintenance was applied, depending on the amount of damage accumulated and the time interval since that activity had last been performed. Overlays were scheduled when the pavement present serviceability index (PSI) fell below 2.5 or when rutting exceeded 1.0 in (2.5 cm).

The roadways tested all had flexible pavements with a structural number of 4.7. This structure was designed according to AASHTO recommendations (5) for simulated traffic of 9300 vehicles per day, imposing an average of 770 equivalent 18-kip axle loads per day. No traffic growth was assumed. Environmental factors specified were typical of northeastern United States: an average rainfall of 10 in (25 cm) per three-month season, a freezing index of 800, and an AASHTO regional factor of 2.5. The asphalt concrete moduli of the pavement surface were varied seasonally as a function of the average seasonal temperature.

Results of the simulations indicated that pavement performance under good and fair drainage conditions was virtually identical. Under poor drainage conditions, however, the rate of pavement damage increased, resulting in worse pavement surface conditions over time and increased pavement-related costs to both the highway agency and road users. If this finding were generally true, it would mean that a minimally acceptable value of subbase permeability lies between the poor and fair values [0.1-100 ft/day (0.03-30.5 m/day)].

Figure 3 illustrates trends in PSI over a 20-year analysis period. The pavements subject to good and fair drainage are overlaid after 13 years in service, their PSI having dropped to 2.5 in that time. The pavement having poor drainage, however, fails after only 9 years' service. The four years' difference in pavement life is due solely to the effects of water infiltration in weakening the sublayers of the pavement with poor drainage, which leads to more rapid damage accumulation.

The trends in pavement damage are indicated in Figures 4 through 6, which show patterns similar to that noted for PSI above. Both roughness and rutting are accelerated in the pavement with poor drainage and are correctable only through overlays. The levels of cracking, however, show no real variation among the three pavements. The reason is that, for this particular simulation, most of the cracking is due to cold-weather shrinkage, which is independent of traffic loads. (Had the cracking been dominated by fatigue mechanisms, the trends likely would have been different between the poor drainage and the other pavements.)

Cracking is reduced to zero in those years in which pavements are overlaid. In other years cracking is allowed to accumulate until it is repaired by routine maintenance on a three-year cycle. (Figure

Figure 3. Serviceability over time.

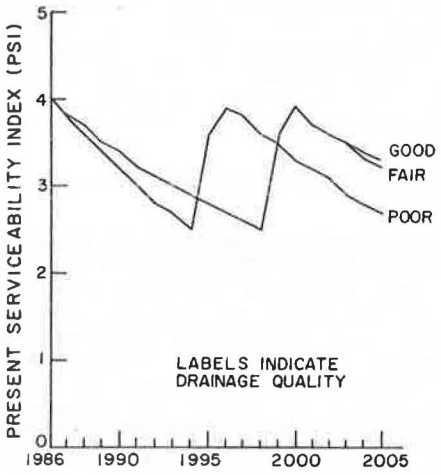

Figure 4. Rutting over time.

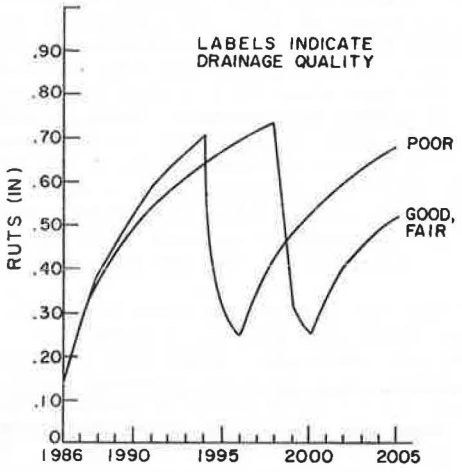

Figure 5. Roughness over time.

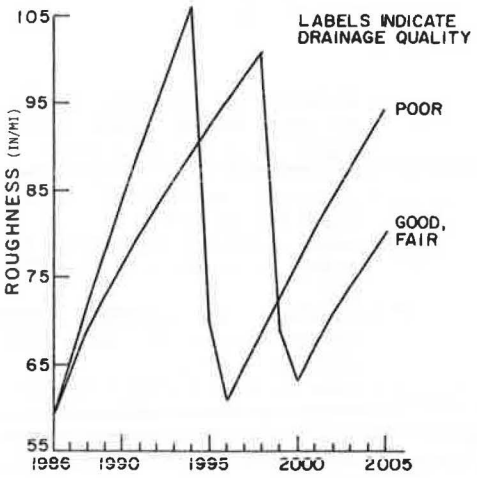

Figure 6. Cracking over time.

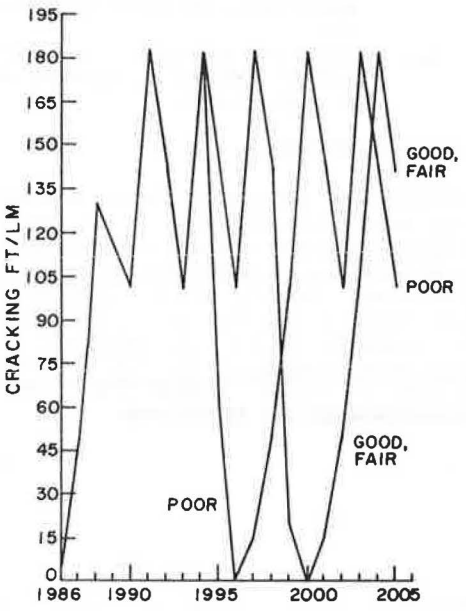

6 shows annual averages of surface cracking. Since some cracks existed at the beginning of those years in which crack filling was performed, the annual average does not reduce to zero in these years, even after maintenance.) Because the cracking in all roadways falls within the same range of values, observed differences in pavement performance are due only to the length of time the pavement sublayers are saturated and not to differences in water inflow.

The ride quality of the pavement surface has effects on road users through influences on speed, travel-time costs, and vehicle-operating costs. Differences in these user costs among pavement policies can in turn be applied to justify, on an economic basis, specific pavement maintenance, rehabilitation, or reconstruction actions. Figure 7 shows the trends in annual user costs for the three pavements tested. As expected, user costs increase more rapidly on the pavement with poor drainage, demonstrating the effects on the motoring public of the damage accumulation.

The fact that the curves for fair and good drainage generally coincide in Figures 3-7 indicates that subbase permeabilities of the order of 100 ft/day (30.5 m/day) already provide adequate drainage for the rainfall amounts and intensities tested. Results for these drainage levels would be expected to diverge as either rainfall amount or daily intensity increased. In fact, we have observed differences in pavement performance and costs for good versus fair drainage in a separate set of simulations that used annual rainfall of 80 in (200 cm) per year, twice those assumed in Figures 3-7. However, the relative benefits for good versus fair drainage are much less than those for fair versus poor drainage, supporting our statement earlier that an acceptable minimum value of coefficient of permeability for the pavement drainage layer lies within the poor to fair range.

The stream of user costs (Figure 7) can be considered with agency expenditures and both streams discounted through the analysis period to conduct an economic analysis based on total costs. Table 2 presents results for the three roadways analyzed by the EAROMAR simulation (exclusive of salvage value). At a 4 percent discount rate (appropriate for constant-dollar analyses), the pavement with fair drainage provides a net benefit of $184 000 and that with good drainage a net benefit of $191 000 through the analysis period. On an economic basis, this is the amount one should be willing to pay to

Figure 7. User costs over time.

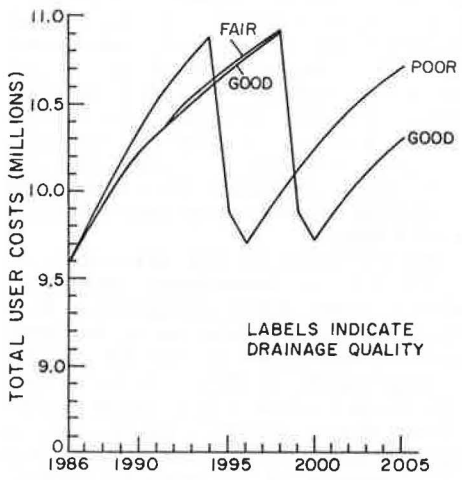

Table 2. Economic analysis of roadways with different drainage characteristics.

	Millions of Dollars				
Quality of Drainage	Overlay Expenditures	Maintenance Expenditures	User Costs	Total Costs	Cost Difference in Relation to Poor Drainage
Good	0.576	0.004	138.838	139.418	0.191
Fair	0.576	0.004	138.845	139.425	0.184
Poor	0.674	0.003	138.933	139.609	–

improve the drainage conditions or maintenance on the poor roadway. Stated another way, if the 10-mile roadway that has poor drainage could be rehabilitated to provide fair to good drainage or could be maintained each year to prevent water infiltration at a cost whose value discounted at 4 percent did not exceed $184 000 to $191 000, this improvement would be economically justified.

CONCLUSIONS

We have presented here an approach to assess the effects of drainage quality on pavement performance and costs. Although the procedure has been applied to date only within a simulation model and must yet be verified in the field, it provides a sound rational basis for organizing information on pavement structure, traffic and environmental loads, and damage accumulation with respect to water infiltration.

The results of our simulations indicate that, for flexible pavements in regions subject to annual rainfall of about 40 in (100 cm), the inclusion of good drainage characteristics within the pavement structure may increase acceptable performance life by about four years. On the other hand, poor drainage characteristics increase rates of rutting and roughness accumulation, decreasing overall pavement condition and increasing user costs for vehicle operation and travel time.

Further research is now under way to test this model for different pavements in different environmental regions and to assess the implications of maintenance policy on rates of damage influenced by water infiltration.

ACKNOWLEDGMENT

The research reported in this paper was supported by the Federal Highway Administration and the U.S. Department of Transportation's University Research Program. I gratefully acknowledge the support of these agencies and wish to thank in particular William J. Kenis, Contract Monitor, for his continued encouragement and assistance.

REFERENCES

1. H.R. Cedergren. Drainage of Highway and Airfield Pavements. Wiley, New York, 1974.
2. M.J. Markow and B.D. Brademeyer. Modification of System EAROMAR: Final Technical Report. FHWA, June 1981.
3. L.K. Moulton. Highway Subdrainage Design. FHWA, Rept. FHWA-TS-80-224, Aug. 1980.
4. H.L. Von Quintus, F.N. Finn, W.R. Hudson, and F.L. Roberts. Flexible and Composite Structures for Premium Pavements, Volume 1: Development of Design Procedure. FHWA, Rept. FHWA-RD-80, Nov. 1980.
5. AASHTO Interim Guide for Design of Pavement Structures. American Association of State Highway and Transportation Officials, Washington, DC, 1972.

Pumping Mechanisms of Foundation Soils Under Rigid Pavements

LUTFI RAAD

Pumping of foundation soils under rigid pavements is a soil structure interaction problem in which the interaction among traffic loads, concrete slab, pavement materials, and water should be considered. Repeated stress induced by moving wheel loads could result in pore-water pressures that reduce the strength and stiffness of underlying soil layers and lead to pumping and loss of foundation support. Pumping mechanisms of granular bases in rigid pavements are investigated in terms of dynamic pore-pressure generation and dissipation. Analyses are performed to study the significance of permeability and compressibility of base materials, loading conditions, and drainage conditions on pumping. Higher pore-pressure values are obtained as a result of decrease in base permeability or increase in its compressibility. The inclusion of lateral drains increases the rate of dynamic pore-pressure dissipation and therefore reduces the pumping potential of the granular base. The efficiency of lateral drains, however, is a function of loading frequency. Higher frequency of loading may not allow enough time for pore-pressure dissipation, which may lead to pumping of the base material. The significance of loss of foundation support on the structural response of the pavement is also studied. Results indicate that loss of foundation support leads to increased stresses and deflections in the concrete slab and therefore hastens its rate of deterioration.

Pumping is known to be a major cause of distress in concrete pavements. It occurs when the pore-water pressure buildup induced by heavy wheel loads is high enough to result in the ejection of material and water through cracks and joints in the pavement slab, causing loss of support and hastening the pavement's rate of deterioration.

Pumping of foundation soils under rigid pavements is a soil structure interaction problem in which the interaction among traffic loads, concrete slab, foundation materials, and water should be considered. Repeated stress states induced by moving wheel loads could result in pore-water pressures that reduce the strength and stiffness of underlying soil layers and lead to pumping and loss of foundation support.

Current design and evaluation techniques of subsurface drainage systems that are used to minimize pumping in pavements are based on the ability of these systems to drain pavement moisture under gravitational flow conditions. Permeability of the structural materials and drainage materials is the essential property that influences water drainage in this case. Loading effects imposed by moving traffic on pore-pressure generation and the effectiveness of subsurface drainage systems in dissipating the dynamic pore-pressure buildup have not yet been considered.

In this paper an attempt will be made to identify pumping mechanisms of granular bases in rigid pavements in terms of dynamic pore-water pressure generation and dissipation under repeated traffic loads. The influence of loading conditions, drainage conditions, and material properties on pumping will be investigated. The significance of pumping and the corresponding loss of foundation support on the structural response of the concrete slab will be illustrated.

DYNAMIC PORE-PRESSURE OBSERVATIONS UNDER RIGID PAVEMENTS

Pumping of foundation soils under rigid pavements is associated with dynamic pore-water pressure development under wheel loads. Repeated stress pulses could result in residual pore-water pressure buildup causing progressive loss of shear strength and stiffness in the underlying soil. Liquefaction of granular materials under the rigid slab occurs when the residual pore-water pressure becomes equal to the initial effective overburden pressure. Additional load repetitions could then result in the ejection of granular materials through cracks and joints in the pavement.

Liquefaction behavior of saturated granular soils has been investigated experimentally under undrained loading conditions by using cyclic triaxial tests (1). Thompson (2) performed repeated-load tests on two-dimensional pavement models consisting of a subgrade and a granular base. A transparent face on the model enabled visual observations of the subgrade and base materials. A high degree of saturation was obtained by soaking the pavements from top and bottom. Under repeated loading conditions, significant movements of the granular particles were observed directly under the loaded area. The entire base course within the loaded area appeared to liquefy and each load application caused a pumping action.

Large-scale tests performed on rigid pavement sections indicate that dynamic pore-water pressure could develop in the granular subbase when the pavement is subjected to repeated loads. Dempsey, Carpenter, and Darter (3) conducted repeated-load tests on two-dimensional rigid pavement models (Figure 1a). The sections were soaked and loaded at a frequency of 15 repetitions/min. Results of peak pore-water pressure (i.e., pore-water pressure at the peak of the load cycle) and residual pore-water pressure (i.e., pore-water pressure at the end of the load cycle) variations in a dense-graded base are shown in Figure 1b. An increase of pore pressure is observed with increase in number of load applications. Water and soil directly beneath the slab seemed to pump up along the sides of the slab and through the joint between the slab and the shoulder. Similar tests performed on open-graded bases showed no evidence of pumping or pore-pressure values in excess of 2 kPa.

Pilot tests were performed at the University of Illinois test track (3) to investigate pore-water pressure development under rigid pavements. This was part of a study entitled Evaluation of Drainage Systems for Pavements, sponsored by the New Jersey Department of Transportation (NJDOT). A test section consisting of 76-mm concrete slab, 76-mm dense-graded base, 102-mm clayey gravel subbase, and a clay subgrade was subjected to a 13.3-kN wheel load application at a frequency of 30 repetitions/min. The dynamic pore-water pressure at the interface between the slab and the base was monitored.

The variation of peak and residual pore pressure is shown in Figure 2. During the first loading sequence, an increase in peak and residual pore-pressure values is observed with increase in number of load repetitions. When loading stops, the residual pore pressure dissipates from 3.90 kPa to 1.70 kPa. Additional loading causes the pore pressure to build up again. In this case, peak pressure values are higher than those observed during the first loading sequence. This could be attributed to the development of voids under the slab and agrees with recent findings by Phu and Ray (4) that an increase in size of the cavity results in higher values of ejection velocity and therefore higher values of peak pore-water pressure.

DYNAMIC PORE-PRESSURE PREDICTIONS UNDER RIGID PAVEMENTS

The development of a pumping model requires an understanding of pore-water pressure development in soils under repeated stress applications similar to those induced by traffic loads. Martin and Seed (5) proposed a method for predicting pore-water pressure generation and dissipation in soils under dynamic loads. The basic assumption involved in their approach is that excess pore-water change in a soil element is the sum of the pore-pressure increment generated by repeated loading and the pore-pressure change due to drainage of water in and out of the element. Assuming one-dimensional flow (i.e., in the direction of the Z-axis) and applying Darcy's law, the basic differential equation for the simultaneous generation and dissipation of pore-water pressure can be written as follows:

$$(\partial u_r/\partial t) = [(1/m_v\gamma_w)(\partial u_r/\partial z)(k\partial u_r/\partial z)] + [(\partial u_g/\partial N)(dN/dt)] \quad (1)$$

where

γ_w = density of water,
u_r = residual pore-water pressure,
m_v = coefficient of volume compressibility,
k = permeability,
N = number of load repetitions,
$(\partial u_g/\partial N)$ = rate of generation of residual pore pressure under undrained loading condition, and
(dN/dt) = frequency of load applications.

Martin and Seed (5) used an implicit finite difference formulation to solve this equation. A com-

puterized form has been developed for pore-pressure predictions under rigid pavements and has been used in this study.

Analyses were performed to investigate dynamic pore-pressure development in soil layers underlying rigid pavements in terms of material properties, loading conditions, and drainage conditions. Stresses were computed in the pavement section and were used as input in pore-pressure prediction under traffic loads.

The finite-element method of analysis was used to determine the stresses in the pavement structure. Nonlinear stress-dependent behavior for the granular base and subgrade was incorporated in the analysis (6). For the granular base, the resilient modulus M_R can be expressed as follows:

$$M_R = K\theta^n \quad (2)$$

where

K, n = material constants,
$\theta = \sigma_1 + \sigma_2 + \sigma_3$, and
$\sigma_1, \sigma_2, \sigma_3$ = principal stresses for the following subgrade:

$$M_R = k_2 - k_3[k_1 - (\sigma_1 - \sigma_3)], \quad k_1 > (\sigma_1 - \sigma_3) \quad (3)$$

and

$$M_R = k_2 + k_1[(\sigma_1 - \sigma_3) - k_1], \quad k_1 < (\sigma_1 - \sigma_3) \quad (4)$$

where k_1, k_2, k_3, and k_4 are material constants. k_3 and k_4 are equal to the rate of change of M_R with repeated deviator stress $(\sigma_1 - \sigma_3)$.

The ratio of maximum shear stress τ_{max}, defined as $[(\sigma_1 - \sigma_3)/2]$, to the initial effective overburden pressure σ_0' was used to estimate the number of cycles required for initial liquefaction N_ℓ obtained from undrained cyclic triaxial tests (5). An example of the variation of N_ℓ with (τ_{max}/σ_0') for a uniform medium sand at different relative densities D_r is shown in Figure 3 (5). The dynamic pressure u_ℓ generated under undrained loading conditions was determined from the following expression (5):

$$u_\ell = \sigma_0' (2/\pi) \arcsin (N/N_\ell)^{(1/2\alpha)} \quad (5)$$

Figure 1. Dynamic pore pressure under rigid slab.

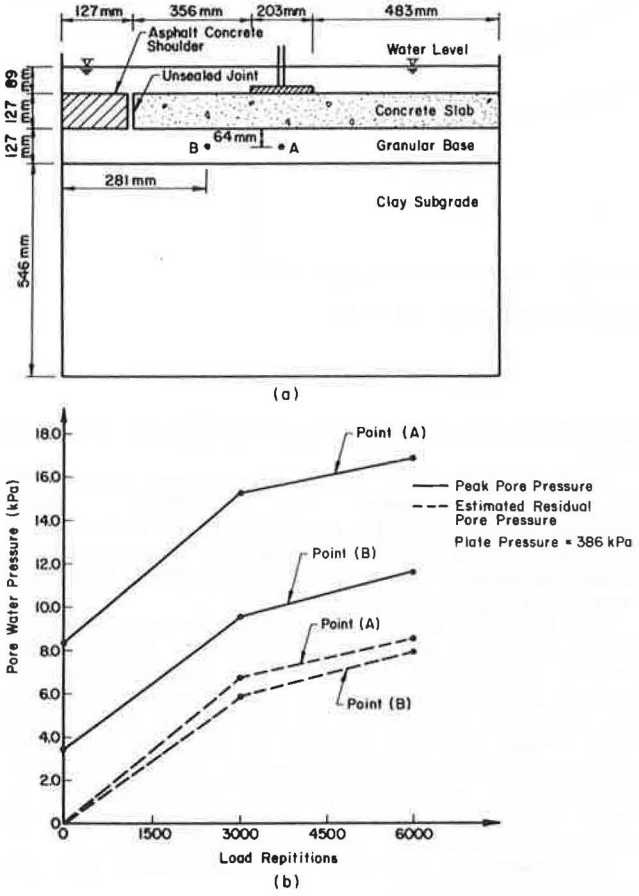

Figure 2. Dynamic pore pressure in dense-graded subbase.

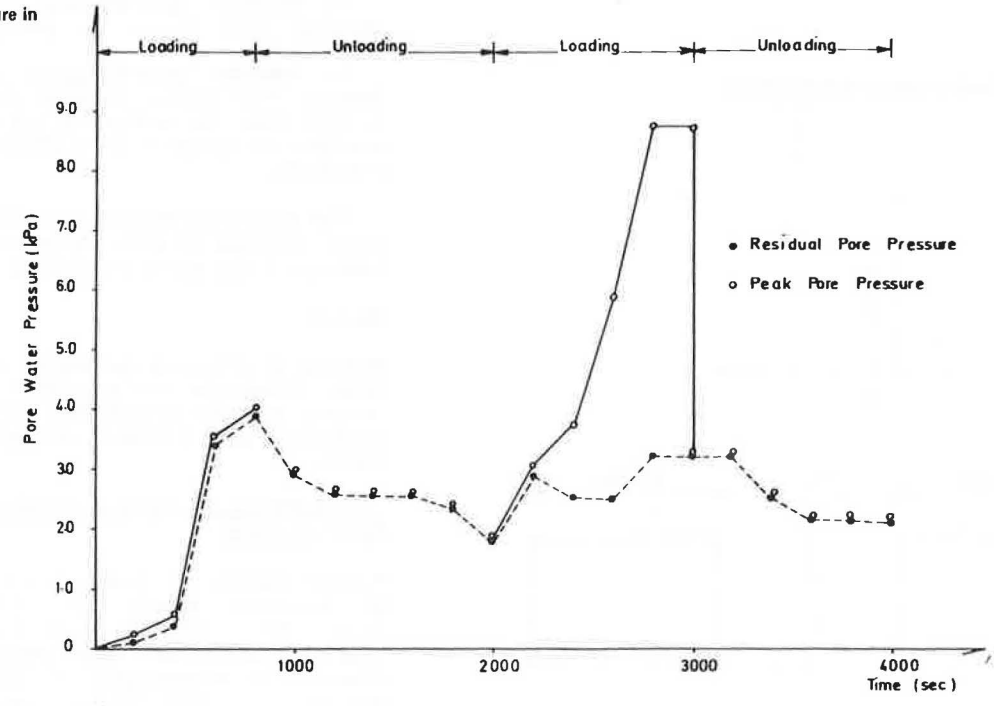

Figure 3. Typical cyclic loading test data.

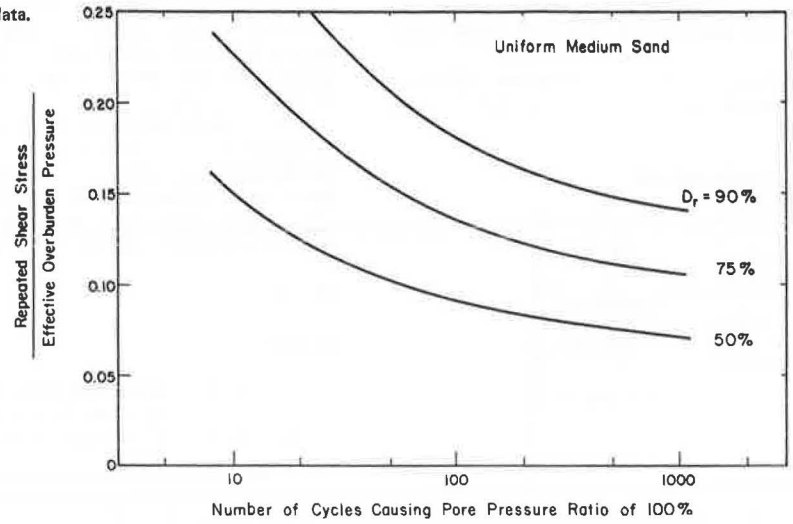

Figure 4. Pavement section analyzed.

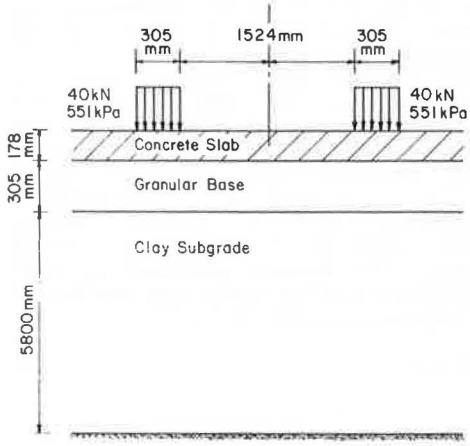

Figure 5. Loading sequence used in analyses.

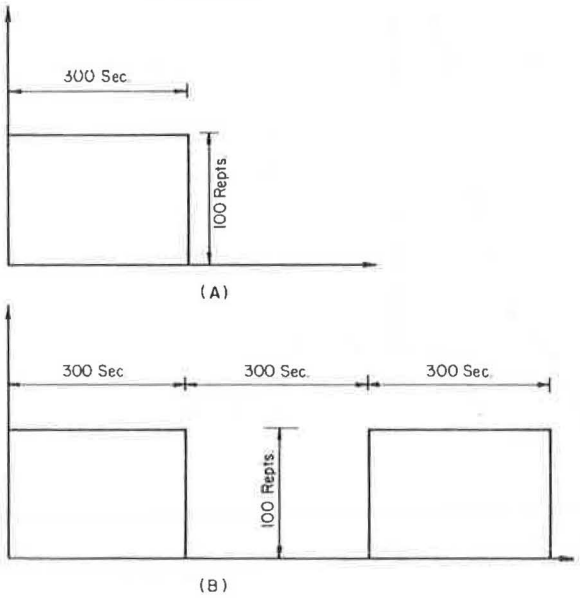

where N is the number of load repetitions and α is 0.70.

Knowing the rate of pore-pressure generation ($\partial u_g/\partial N$), frequency of applied loads (dN/dt), coefficient of permeability k, and coefficient of volume compressibility m_v, Equation 1 was solved to obtain the dynamic pore-pressure distribution under rigid pavements.

The pavement section considered in this study is shown in Figure 4. The pavement was subjected to loading sequences A and B of 80-kN single-axle loads applied at a frequency of 20 repetitions/min (Figure 5). Sequence A consists of one series of 100-load repetitions, whereas sequence B includes two such series applied at 300-s intervals. Material properties used in stress computations are summarized in Table 1. The variation of (τ_{max}/σ_0') in the pavement section is illustrated in Figure 6.

Pore-pressure analyses were performed for the following conditions:

1. Dynamic pore-pressure dissipation through vertical flow (i.e., no lateral drainage is allowed); and
2. Dynamic pore-pressure dissipation through lateral flow (i.e., lateral drainage is allowed). In this case the efficiency of subsurface drains in dissipating dynamic pore-water pressure could be evaluated.

The finite-difference representation of the sections analyzed is illustrated in Figures 7 and 8. A summary of the cases studied is presented in Table 2.

RESULTS

Results of analyses presented in the following sections illustrate the significance of material properties, loading conditions, and drainage conditions on dynamic pore pressure and pumping in rigid pavements.

Pore-Pressure Dissipation Through Vertical Flow

Dynamic pore-water pressure was calculated assuming pore-pressure dissipation through vertical flow (i.e., no lateral drainage was allowed). Higher pore-pressure values were obtained as a result of decrease in permeability of the granular base. For example, a pore-pressure ratio [i.e., u_r/σ_0']

equal to unity will develop if the permeability decreases from 10^{2} to 10^{-2} cm/s (Figure 9, cases 1 and 2). In this case the pore pressure becomes equal to the initial effective overburden pressure and a condition of initial liquefaction will occur, thereby increasing the susceptibility of the granular base to pumping. Similar behavior is observed for higher compressibility of the base (cases 2 and 3) or larger number of load repetitions (cases 2 and 4).

The effect of permeability and compressibility of

Table 1. Material properties used in stress predictions.

Material	Resilient Properties	Failure Criteria	Density (kg/m^3)
Concrete	$E = 34.5 \times 10^6$ kPa $\nu = 0.10$	—	2400
Base course	$K = 6495$ $n = 0.60$ $\nu = 0.30$	$C = 0$ $\phi = 30^0$	2130
Subgrade	$k_1 = 41.3$; $k_2 = 41\,300$ $k_3 = 0.300$; $k_4 = -75$ $\nu = 0.45$	$C = 90$ kPa $\phi = 0^0$	1950

Notes: Saturated unit weights are used for base course and subgrade. K,n are parameters for resilient modulus of base course (Equation 2). k_1, k_2, k_3, k_4 are parameters for resilient modulus of subgrade (Equations 3 and 4). Resilient moduli of base and subgrade are expressed in kilopascals. E and ν are elastic modulus and Poisson's ratio, respectively.

Figure 6. Variation of maximum shear with depth under center of wheel load.

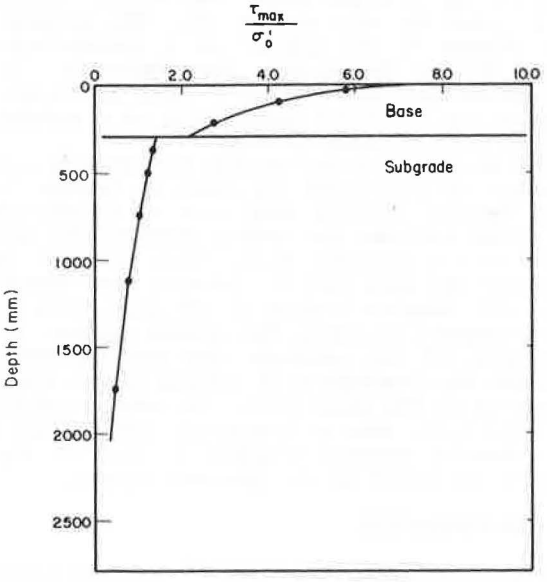

Figure 7. Finite difference representation for vertical flow condition.

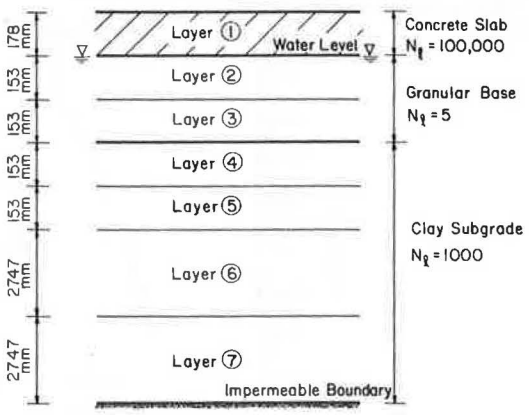

Figure 8. Finite difference representation for lateral flow condition.

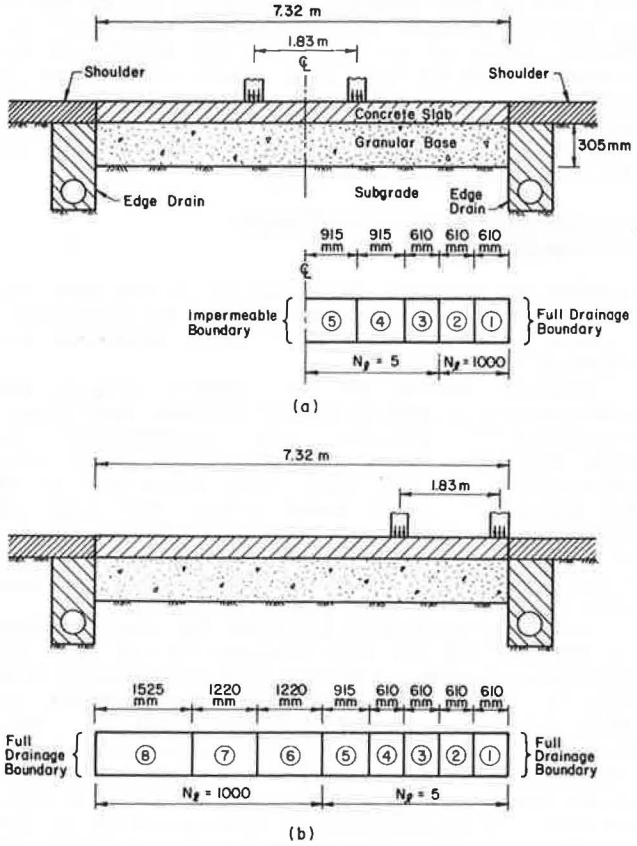

Table 2. Pavement systems analyzed.

Case	Concrete k (cm/s)	Concrete m_v (m^2/kN)	Base Course k (cm/s)	Base Course m_v (m^2/kN)	Subgrade k (cm/s)	Subgrade m_v (m^2/kN)	Loading Sequence	Drainage Condition
1	10^{-8}	2.0×10^{-7}	10^{-2}	2.0×10^{-5}	10^{-8}	2.0×10^{-4}	A	Vertical flow
2	10^{-8}	2.0×10^{-7}	10^{-2}	2.0×10^{-5}	10^{-8}	2.0×10^{-4}	A	
3	10^{-8}	2.0×10^{-7}	10^{-2}	2.0×10^{-4}	10^{-8}	2.0×10^{-4}	A	
4	10^{-8}	2.0×10^{-7}	10^{-2}	2.0×10^{-5}	10^{-8}	2.0×10^{-4}	B	
5	—	—	10^{-1}	2.0×10^{-5}	—	—	A	Lateral flow (interior loading)
6	—	—	10^{-2}	2.0×10^{-5}	—	—	A	
7	—	—	10^{-2}	2.0×10^{-4}	—	—	A	
8	—	—	10^{-2}	2.0×10^{-4}	—	—	B	
9	—	—	10^{-1}	2.0×10^{-5}	—	—	A	Lateral flow (edge loading)
10	—	—	10^{-2}	2.0×10^{-5}	—	—	A	
11	—	—	10^{-2}	2.0×10^{-4}	—	—	A	
12	—	—	10^{-2}	2.0×10^{-4}	—	—	B	

Note: Relative density D_r of granular base is 85 percent.

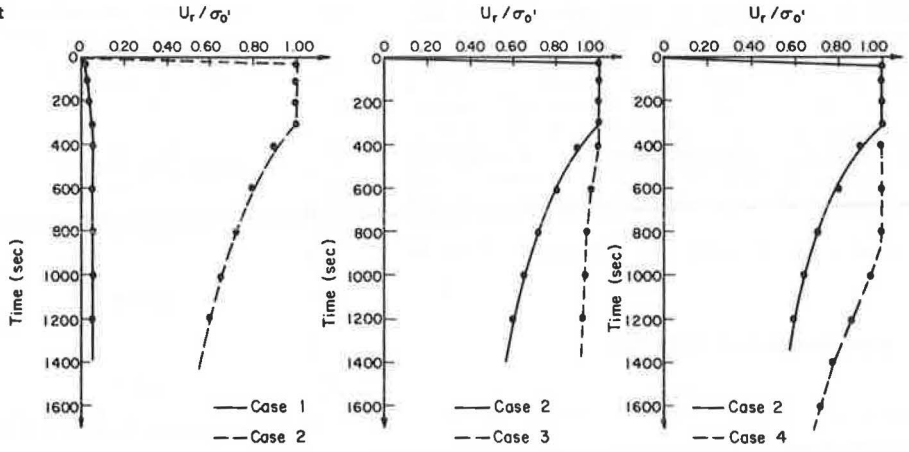

Figure 9. Dynamic pore pressure at top of granular base for pavement with no lateral drainage.

the base on pore-pressure dissipation at the end of a loading sequence is illustrated in Figure 10. Higher values of pore pressure are maintained for longer periods of time as a result of decrease in base permeability or increase in its volume compressibility. This would increase the pumping potential of the base if the pavement is subjected to an additional sequence of loads.

Pore-Pressure Dissipation Through Lateral Flow

Results of analyses performed to investigate the effectiveness of subsurface drains in dissipating dynamic pore pressure under rigid pavements are shown in Figures 11-14.

Interior loading of the pavement (Figure 11) could result in pumping of the granular base [i.e., $(u_r/\sigma_0') = 1$] provided its permeability is less than 10^{-2} cm/s. An increase in volume compressibility of the base from 2.0×10^{-3} m²/kN to 2.0×10^{-4} m²/kN would reduce the rate of pore-pressure dissipation as illustrated in Figures 11 and 12 (cases 6 and 7). Additional load applications would increase the pore pressure in the base and may cause additional pumping (Figure 12c).

Similar observations are made for loads applied at the edge of the slab (Figures 13 and 14). In this case, however, a reduction in permeability from 10^{2} to 10^{-2} cm/s would not cause pumping as shown in Figures 13 and 14 (cases 9 and 10). This could be attributed to the effectiveness of subsurface drains in dissipating the dynamic pore pressures induced by such loading conditions. If this reduction in permeability is accompanied by an increase in volume compressibility to a value of 2.0×10^{-4} m²/kN, then the pore-pressure ratio would increase from 0.3 to 1.0 (Figures 13c and 14b) and pumping of the granular base could occur.

The effectiveness of subsurface drains in dissipating dynamic pore pressure and therefore in reducing pumping potential is illustrated by comparing results in Figures 9 and 12. For the same material properties and loading conditions, the rate of pore-pressure dissipation is greater for pavements with subsurface drains.

The efficiency of subsurface drains depends to a certain extent on the frequency of load applications. A decrease in frequency of loading would increase the time span between load applications, thereby allowing more time for pore-pressure dissipation. Higher frequency of loading may not allow enough time for pore-pressure dissipation and therefore could lead to initial liquefaction and pumping.

STRUCTURAL EFFECTS

The development of excess pore-water pressure under rigid pavements reduces the effective stresses and leads to a decrease in shear strength and stiffness of pavement materials. Loss of foundation support could result from increased permanent deformations or pumping of foundation material through cracks and joints in the pavement.

Analyses were performed to investigate the effect of loss of foundation support on the structural response of the concrete slab. The finite-element method was used for this purpose (7). The pavement section (Figure 5) was modeled as a medium-thick plate on a Winkler foundation. The modulus of subgrade reaction used was 52 MN/m³. Loss of foundation support was simulated analytically by a modulus of subgrade reaction equal to zero.

Tensile stresses and deflections for interior and edge-loading (8) conditions are shown in Figures 15 and 16. Results indicate that loss of foundation support would increase the tensile stresses and deflections in the pavement slab. This increase is more critical for edge than for interior load applications. For interior loading of the slab, loss of foundation support increases the tensile stresses on the underside of the pavement slab and therefore could hasten the development of fatigue cracks along the direction of the wheel path. For edge loading, on the other hand, loss of foundation support could induce excessive tensile stresses on top of the slab, which may result in edge punchout failure.

SUMMARY AND CONCLUSIONS

In this paper, pumping mechanisms of granular bases in rigid pavements have been investigated in terms of dynamic pore-water pressure generation and dissipation under repeated traffic loads. Dynamic pore-pressure development reduces shear strength and stiffness of underlying soil layers. Liquefaction of saturated granular materials under the rigid slab occurs when the residual pore-water pressure becomes equal to the initial effective overburden pressure. Additional load repetitions could then result in the ejection of base material through cracks and joints in the pavement.

Analyses were performed to study the significance of permeability and compressibility of base materials, loading conditions, and drainage conditions on pumping. Higher pore-pressure values were obtained as a result of a decrease in base permeability or an increase in its compressibility. The inclusion of lateral drains increases the rate of dynamic pore-

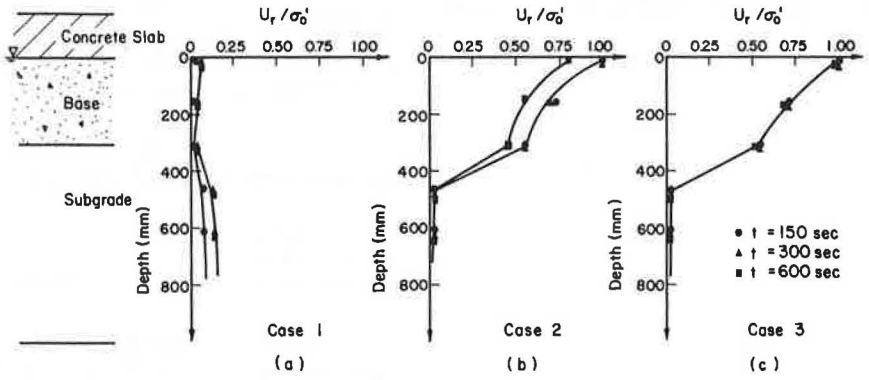

Figure 10. Dynamic pore-pressure variation below center of wheel load for pavement with no lateral drainage.

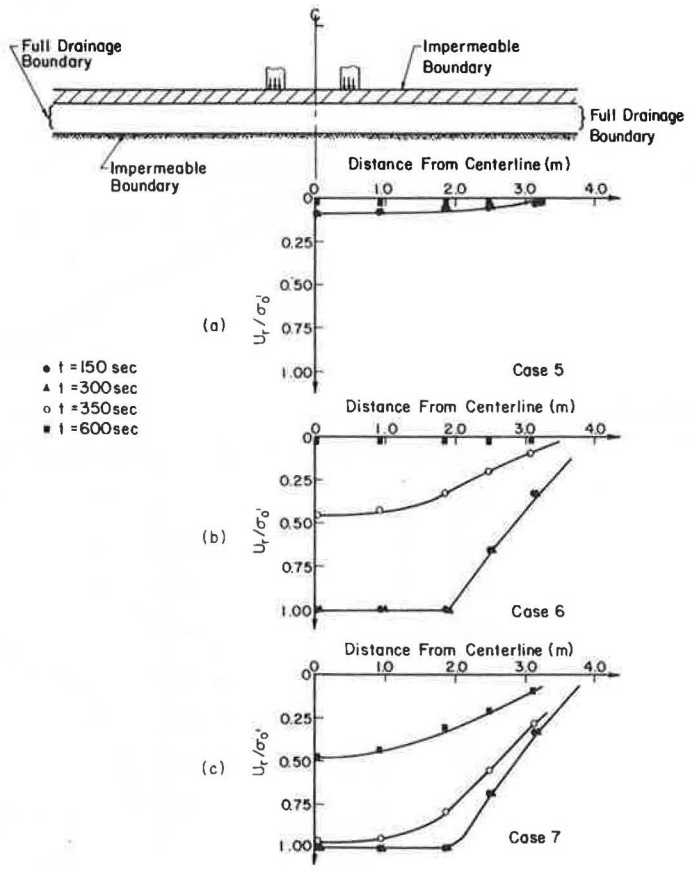

Figure 11. Pore-pressure variation for interior loading of slab.

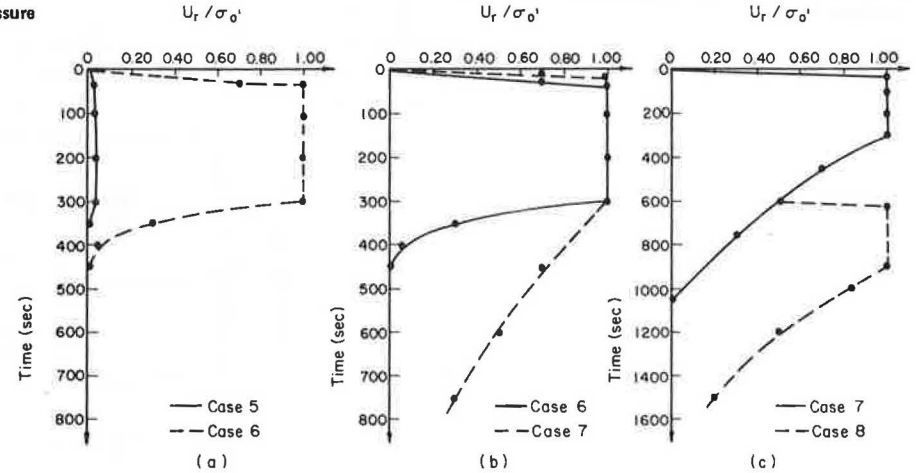

Figure 12. Variation of maximum pore pressure in base for interior loading of slab.

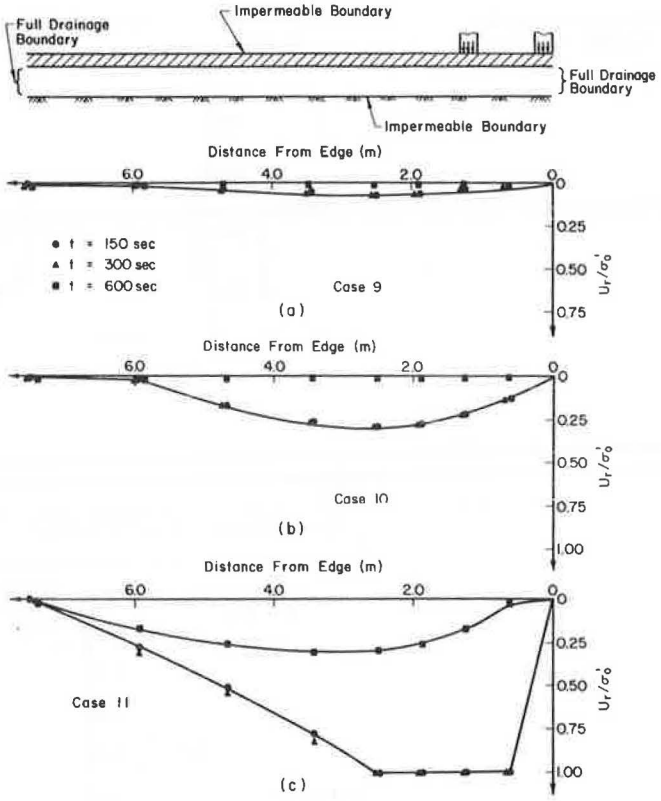

Figure 13. Pore-pressure variation for edge loading of slab.

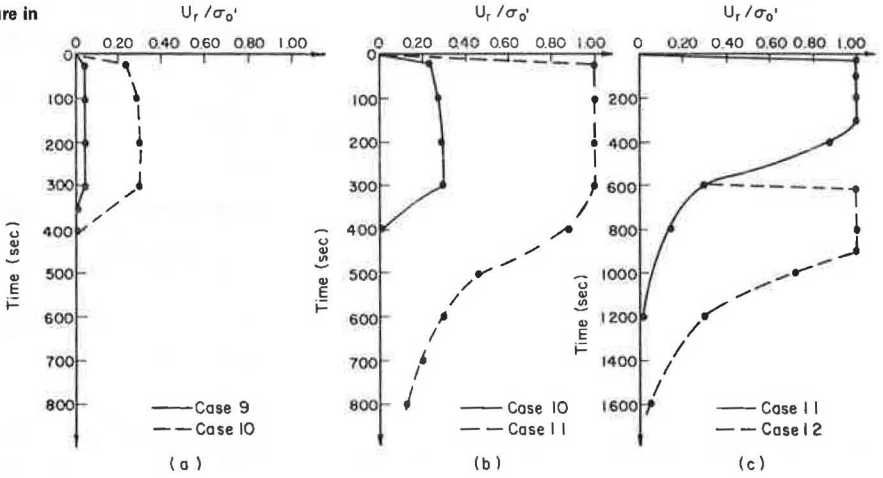

Figure 14. Variation of maximum pore pressure in base for edge loading of slab.

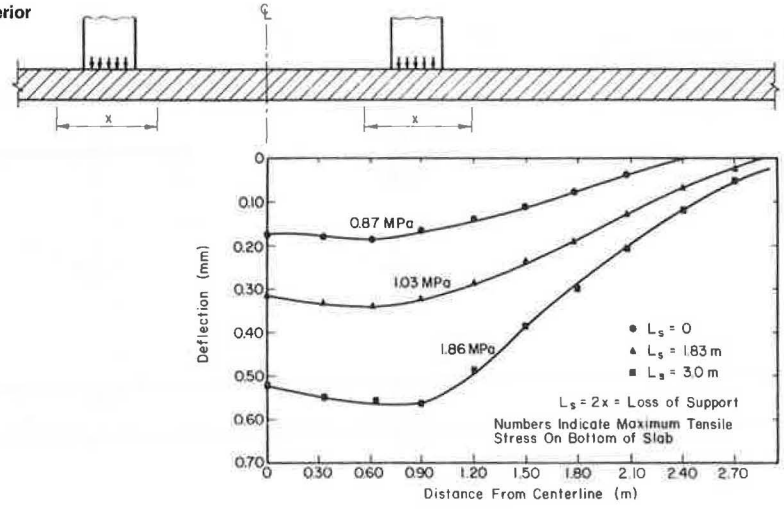

Figure 15. Effect of loss of support on slab response for interior loading condition.

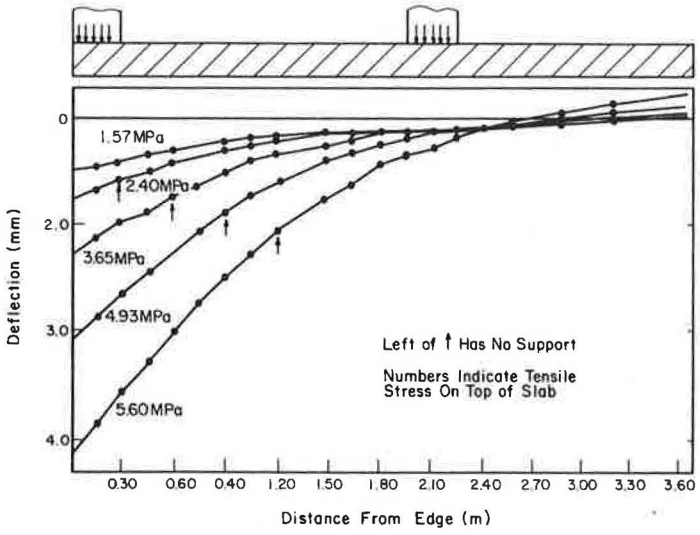

Figure 16. Effect of loss support on slab response for edge loading condition.

pressure dissipation and therefore reduces the pumping potential of the granular base. The efficiency of lateral drains, however, is a function of loading frequency. Higher frequency of load applications would not allow enough time for pore-pressure dissipation, which could lead to pumping of base material.

Results of analyses indicate that loss of foundation support caused by pumping and permanent deformations of soil layers under the pavement would result in increased stresses and deflections in the concrete slab and therefore would hasten its rate of deterioration.

ACKNOWLEDGMENT

This investigation was conducted at the University of Illinois at Urbana-Champaign. I appreciate the assistance of B.J. Dempsey and E.J. Barenberg in conducting the pilot tests at the University of Illinois test track. Special thanks go to P.P. Martin and H.Y. Chu for their help during the analytical studies.

REFERENCES

1. H.B. Seed and K.L. Lee. Liquefaction of Saturated Sands During Cyclic Loading. Journal of Soil Mechanics and Foundation Engineering of ASCE, Vol. 92, No. SM6, Nov. 1966, pp. 105-134.
2. O.O. Thompson. Evaluation of Flexible Pavement Behavior with Emphasis on the Behavior of Granular Layers. Department of Civil Engineering, Univ. of Illinois at Urbana-Champaign, Ph.D. thesis, 1969.
3. B.J. Dempsey, S.H. Carpenter, and M.I. Darter. Improving Subdrainage and Shoulders of Existing Pavements. FHWA, Final Rept., Aug. 1980.
4. N.C. Phu and M. Ray. Hydraulique du Pompage des Chaussees en Beton Premier Bilan de l'Approche Theorique et des Resultats de Mesure en Laboratoire et sur Autoroute. Chaussées en Beton, Laboratoire Central des Ponts et Chaussées, Paris, 1979, pp. 15-31.
5. P.P. Martin and H.B. Seed. APOLLO: A Computer Program for the Analysis of Pore Pressure Generation and Dissipation in Horizontal Sand Layers During Cyclic or Earthquake Loading. Univ. of California, Berkeley, Rept. UCB/EERC-78/21, Oct. 1978.
6. L. Raad and J.L. Figueroa. Load Response of Transportation Support Systems. Transportation Engineering Journal of ASCE, Vol. 106, No. TE1, Jan. 1980, pp. 111-128.
7. A.M. Tabatabaie, E.J. Barenberg, and R.E. Smith. Analysis of Load Transfer Systems for Concrete Pavements, Volume 2: Analysis of Load Transfer Systems in Concrete Pavements. Federal Aviation Administration, U.S. Department of Transportation, 1979.
8. S.A. LaCoursiere, M.I. Darter, and S.A. Smiley. Performance of Continuously Reinforced Concrete Pavements in Illinois. FHWA, Rept. FHWA-IL-UI-112, Dec. 1979.